

**Enhancement of Near-Real-Time
Cloud Analysis
And Related Analytic Support
For Whole Sky Imagers**

**Final Report for ONR Contract
N00014-01-D-0043 DO #4**

UNIVERSITY
OF
CALIFORNIA
SAN DIEGO



SCRIPPS
INSTITUTION
OF
OCEANOGRAPHY

Janet E. Shields

Monette E. Karr

Art R. Burden

Richard W. Johnson

William S. Hodgkiss

MARINE PHYSICAL LAB San Diego, CA 92152-6400

Report Documentation Page				Form Approved OMB No. 0704-0188	
Public reporting burden for the collection of information is estimated to average 1 hour per response, including the time for reviewing instructions, searching existing data sources, gathering and maintaining the data needed, and completing and reviewing the collection of information. Send comments regarding this burden estimate or any other aspect of this collection of information, including suggestions for reducing this burden, to Washington Headquarters Services, Directorate for Information Operations and Reports, 1215 Jefferson Davis Highway, Suite 1204, Arlington VA 22202-4302. Respondents should be aware that notwithstanding any other provision of law, no person shall be subject to a penalty for failing to comply with a collection of information if it does not display a currently valid OMB control number.					
1. REPORT DATE 30 MAY 2007		2. REPORT TYPE		3. DATES COVERED	
4. TITLE AND SUBTITLE Enhancement of Near-Real-Time Cloud Analysis and Related Analytic Support for Whole Sky Imagers				5a. CONTRACT NUMBER	
				5b. GRANT NUMBER	
				5c. PROGRAM ELEMENT NUMBER	
6. AUTHOR(S) Janet Shields; Monette Karr; Art Burden; Richard Johnson; William Hodgkiss				5d. PROJECT NUMBER	
				5e. TASK NUMBER	
				5f. WORK UNIT NUMBER	
7. PERFORMING ORGANIZATION NAME(S) AND ADDRESS(ES) Marine Physical Laboratory, Scripps Institution of Oceanography/University of California, San Diego, 291 Rosecrans St., San Diego, CA, 92106				8. PERFORMING ORGANIZATION REPORT NUMBER MPL TM-	
9. SPONSORING/MONITORING AGENCY NAME(S) AND ADDRESS(ES)				10. SPONSOR/MONITOR'S ACRONYM(S)	
				11. SPONSOR/MONITOR'S REPORT NUMBER(S)	
12. DISTRIBUTION/AVAILABILITY STATEMENT Approved for public release; distribution unlimited.					
13. SUPPLEMENTARY NOTES					
14. ABSTRACT This report describes the research performed on behalf of the Office of Naval Research (grant # N00014-01-D-0043 Delivery Order 0004) on the following: Enhancement of Near-Real-Time Cloud Analysis and Related Analytic Support for Whole Sky Imagers					
15. SUBJECT TERMS					
16. SECURITY CLASSIFICATION OF:			17. LIMITATION OF ABSTRACT 2	18. NUMBER OF PAGES 49	19a. NAME OF RESPONSIBLE PERSON
a. REPORT unclassified	b. ABSTRACT unclassified	c. THIS PAGE unclassified			

Enhancement of Near-Real-Time Cloud Analysis And Related Analytic Support For Whole Sky Imagers

Table of Contents

1. Introduction.....	1
2. Background.....	1
3. Statement of Work	2
4. Funding Increments and Optional Tasks	4
5. Major Deliveries and Documentation.....	5
6. Discussion of Hardware Developments.....	8
7. Day Algorithm Developments and Analysis	10
8. Night Algorithm Developments and Analysis.....	16
9. Discussion of Wavelength Options for Optical Cloud Imaging	20
9.1 The Visible and SWIR Intercomparison Experiment	21
9.2 Thermal IR Systems	24
9.3 Comments Regarding Mid Wave IR Systems	25
9.4 Theoretical Study of LWIR Characteristics	26
9.4.1 Discussion of the Approach	26
9.4.2 Cloud Signatures, part 1.....	27
9.4.3 Background Signatures	29
9.4.4 Cloud Signatures, part 2.....	31
9.4.5 Resulting Cloud and Background Effective Temps....	32
9.5 Summary of the Wavelength Analysis	34
10. Summary.....	35
11. Acknowledgements	35
12. References	36

List of Illustrations

Fig. 1	Profile of Standard WSI Occultor.....	9
Fig. 2	Profile of Improved Occultor.....	9
Fig. 3	Initial Design for computer control to replace ACP Panel.....	11
Fig. 4	Raw Red and Processed Cloud Decision for 20 Feb 02 1420	12
Fig. 5	Raw Red and Processed Cloud Decision for 21 Feb 02 1700	12
Fig. 6	Raw Red and Processed Cloud Decision for 12 Aug 02 1706 ...	13
Fig. 7	Raw Red and Processed Cloud Decision for 16 Aug 02 2200 ...	13
Fig. 8	Forward Bias Haze Case.....	13
Fig. 9	Reverse Bias Haze Case	13
Fig. 10	Red/Blue Ratio Through the Sun on 3 Typical Days	14
Fig. 11	Red/Blue Ratio Through the Sun on Forward Bias Days	15
Fig. 12	Red/Blue Ratio Through the Sun on Reverse Bias Days	15
Fig. 13	No Moon Case in Oklahoma	16
Fig. 14	No Moon Case at SOR enhanced to show clds away from city	16
Fig. 15	No Moon Case at SOR enhanced to show clds near city	17
Fig. 16	Moonlight Example	17
Fig. 17	Night Raw and Processed Data for a clear case.....	17
Fig. 18	Night Raw and Processed Data for a broken cloud case	18
Fig. 19	Night Raw and Processed Data for an overcast case	18
Fig. 20	Star Irradiance Comparison	19
Fig. 21	Sample Cloud Transmittance ExtractionResults	20
Fig. 22	Overcast case, imagery at 1.6 μ m and 650 nm	22
Fig. 23	Thin clouds, imagery at 1.6 μ m and 650 nm	22
Fig. 24	Thin and pre-emergent clouds at 1.6 μ m and 650 nm	23
Fig. 25	Sunset, imagery at 1.6 μ m and 650 nm.....	23
Fig. 26	Sample Cloud Image taken in the 3 - 5 μ m region	25
Fig. 27	Sample Cloud Image taken in the 8 - 12 μ m region	25
Fig. 28	Vertical Profile of Scattering Coefficients.....	28

Tables

Table 1	Cloud Altitudes used in Calculations.....	27
Table 2	Estimated Vertical Beam Transmittance	29
Table 3	Effective Radiating Temperatures used for Sky Backgrounds.....	31
Table 4	Computed Cloud and Background Results for the Zenith.....	32
Table 5	Computed Cloud and Background Results for 60° Zenith Angle..	33
Table 6	Computed Cloud and Background Results for 85° Zenith Angle..	33

Enhancement of Near-Real-Time Cloud Analysis And Related Analytic Support For Whole Sky Imagers

**Janet E. Shields, Monette E. Karr,
Art R. Burden, Richard W. Johnson, and William S. Hodgkiss**

1. Introduction

This report describes the work done for the Starfire Optical Range, Kirtland Air Force Base under Contract N00014-01-D-043 DO #4, between 25 May 01 and 31 September 06. This work relates to the Air Force's need to characterize the cloud distribution during day and night, for a variety of applications, including support of satellite tracking, and support of research into impact of clouds on laser communication. This contract followed Contract N00014-97-D-0350 DO #6, which will be discussed in Section 2, and is documented in Shields et al 2004b, Technical Note 265. The primary goals of Delivery Order #4 discussed in this current report included further development of day and night cloud algorithms and support of the fielded Whole Sky Imager instruments. Much of the work done under DO #4 was completed by the end of 2004. Some additional work was done in 2005 and 2006 under the DO #4 funding, but most of the SOR work during this interval was done under a follow-on contract, ONR N00014-01-D-0043 DO #11, funded September 04. The work under DO #11 will be reported under a separate report.

We would also like to note that we were funded by several other sponsors during this period. Although we have no desire to provide an overview of the other work, in some cases it was related to the SOR goals, and may be discussed in this context.

2. Background

A series of digital, automated Whole Sky Imagers (WSI) have been developed by MPL over many years, beginning in the early 1980's (Johnson et al. 1989 and 1991, and Shields et al. 1993, 1994, 1997a and b). These systems are designed to acquire accurate imagery of the full upper hemisphere in several spectral filters, in order to be able to assess the presence of clouds at each pixel in the image. A system capable of 24-hour operation, the Day/Night WSI, was developed by MPL under funding from the Air Force, Navy, and Army in the early 1990's (Shields et al. 1998, 2003b and e, 2004 a and b, and 2005b and c). One of the first two units was fielded at the Air Force's Starfire Optical Range in October 1992.

Related systems have been designed and fielded over the years. These include a new Daytime Visible/NIR WSI (Feister et al. 2000, and Shields et al. 2003d), and visible and Short-wave NIR systems for airborne use (Shields et al. 2003c). An imaging system for measuring visibility was developed and successfully tested (Shields et al. 2005a and

2006). Also, a field calibration device for use with the Day/Night WSI was developed (Shields et al. 2003a).

Partly as a result of SOR's experience with the Day/Night WSI fielded in 1992, they have funded fabrication of additional instruments, as well as algorithm development and data analysis in recent years. Under Contract N00014-97-D-0350 DO #2 (Sep 97 – June 01), MPL was funded to develop and provide a new Day/Night WSI, which was designated Unit 12 (Shields et al. 2003b). This unit included several design upgrades developed for other sponsors. The funding also included analysis and processing of existing daytime cloud decision images to provide statistical estimates of Cloud Free Line of Sight (CFLOS) and related properties. Under the optional funding, the WSI was also upgraded to run under Windows. This was a major upgrade, involving a new camera model, a new camera software library, and new WSI instrument control software. The instrument was delivered in Jan '99, and has been running well for much of the time since. The data analysis results were also delivered in '98 and '99, and my understanding is that these data have proven to be quite useful.

Under Contract N00014-97-D-0350 DO #6 (May 99 – May 03), we were funded to provide two additional instruments, Units 13 and 14 and do analysis work (Shields et al. 2004b). These instruments included significant design upgrades, including integration of the control computer into the outdoor environmental housing, new control hardware and software, and new software to provide near-real-time cloud processing on an additional display computer. One of the instruments was fielded at a site in California for an experiment, and ran well prior to the completion of the experiment, at which time it was returned to MPL. The other system was kept at MPL pending sponsor readiness for deployment. It was allowed to run continuously, and ran well.

In addition, under the options, we were funded to develop a new Starlight Cloud Algorithm based on detection of the contrast between the signal from stars and their background. The concepts had been developed under funding from another sponsor (Shields et al. 2002), and under Delivery Order 6, this concept was expanded to handle moonlight, and converted to a fieldable C-code. The appropriate geometric calibrations and background were extracted for the Unit 12 running at the SOR site, and the algorithm was installed and provided reasonable results.

Toward the end of this prior contract, a funding increment was received that partially funded the new contract, and partially funded the existing contract. The Statement of Work (SOW) for the new contract, DO #4, reflected the priorities at the time of the funding increment. However, we were asked to use the options under the existing contract, DO #6, to begin the work. The part of this work that was completed under the older contract was reported in Shields et al. 2004b, but it will also be reviewed in Section 5.

3. Statement of Work

The Statement of Work for the Delivery Order #4 is given in italics below.

Primary Task:

The contractor shall, unless otherwise specified herein, supply the necessary personnel, facilities, services, and materials to accomplish the following tasks within a one-year period following receipt of funding.

- 1. Modify the SOR unit, Unit 12, to provide the current version of the night algorithm, Near Infra-Red data acquisition, and cloud algorithm processing on a sponsor-supplied display computer.*
- 2. Provide those miscellaneous software upgrades, such as a modification of the Display Computer interface, which are mutually agreed upon by the sponsor and by MPL to be appropriate.*
- 3. Continue development of the day and/or night cloud algorithm.*
- 4. Provide a stand-alone image processing program, which may be used to process archived data through the cloud algorithms.*
- 5. Provide a final written report and interim verbal reports to the sponsor regarding the results of the above work.*
- 6. Other work such as minor repairs to the instrument are permissible under this task, if they are mutually agreed upon by the sponsor and by MPL to be appropriate. In this case, the work toward the other requirements in this statement of work would be lessened accordingly.*

Optional Task

The contractor shall, unless otherwise specified herein, supply the necessary personnel, facilities, services, and materials to accomplish the following tasks within a two-year period following receipt of funding.

- 1. Coordinate with the sponsor regarding the most appropriate tasks and estimated costs for development.*
- 2. Provide personnel trained in the Whole Sky Imager and its capabilities to address these tasks (at MPL) to the limit of funding provided under the contract. These tasks may include analysis, software development, documentation, minor hardware development, and other tasks related to the WSI that are mutually agreed upon by the sponsor and by MPL to be appropriate.*
- 3. Provide a final written report and interim verbal reports to the sponsor regarding the results of the above work.*

4. Funding Increments and Optional Tasks

The funding was sent from the Air Force to ONR in a number of funding increments, and the optional tasks were defined as these funding increments were received. The funding increments and associated tasks are listed below.

An initial funding increment was sent to ONR in Nov 00. Some of these funds were allocated into the previous Contract N00014-97-D-0350 DO #6, and the remaining funds were put into the new Contract N00014-01-D-043 DO #4. The new contract was received about May 01. The priorities were to work on the tasks listed in the Statement of Work Primary Tasks section. Because we were asked to work on the new priorities under the existing contract, we were able to complete portions of the first two items in the SOW under the earlier contract with this first split funding increment.

The second funding increment was received about Aug 03. This completed funding for the Primary Tasks. In addition, we were given the following priorities under the options.

1. Unit 12 at SOR had been hit by lightning, and we were asked to assess and if possible repair this unit.
2. Deploy Unit 14 to a site in Virginia.

In January 04, we received two additional small funding increments, with the associated tasks given below. At that time, we were asked to keep track of these increments separately because they came from separate funding sources, and so separate budgets were set up. However, later we were told that this was no longer necessary. Thus in this report, we do not distinguish between these different budgets.

3. Continue night transmittance map development and analysis work.
4. Begin to evaluate optimal WSI designs for the future, including hardware, software, and algorithms, and evaluate costs technical and cost tradeoffs associated with providing such instruments.

A fifth funding increment was received Mar 04. The priorities for this increment were:

5. Repair the occulter trolley that had failed on Unit 14, which was fielded in Virginia.
6. For Unit 14, radiometrically calibrated the camera system from Unit 13, and swap it into Unit 14.
7. Provide a glass dome and heater for Unit 14 to minimize dew on the outside of the dome.
8. Evaluate night imagery from Unit 14, which was fielded at a very bright location, and adjust the flux control algorithm to acquire on-scale data.

A sixth funding increment was received on May 04. Part of the funding increment was applied to this contract, and the remaining funds were applied to a new contract, Contract N00014-01-D-043 DO #11, which was received Sep 04 and will be discussed in a separate report. The priorities were for the full funding increment, and thus could be addressed either under this contract or under the follow-on contract. Of these new priorities, the one addressed under this contract is as follows:

9. Evaluate the pros and cons of eventually developing an IR WSI for detecting clouds during the day and at night.

5.0. Major Deliveries and Documentation

All funded tasks were completed. Because there were so many primary and optional tasks, we would like to document the major deliveries and documentation for these tasks. In the later sections, we will provide an overview of the more significant advances related to general capabilities. Additional documentation is provided in the technical memoranda listed below and in the reference section. These technical memos can be provided to the sponsor upon request.

Primary Task 1: In January 01, we took a trip to SOR to upgrade the WSI Unit 12. The system was upgraded to include a Near Infrared (NIR) filter, to better handle haze and thin clouds. A processing computer was added to the system, to enable real-time processing of the cloud algorithm. Changes were made to the data acquisition software to enable both of these upgrades, and a new processing program, to enable running both the day and night algorithms, was written and installed. (This program, like the earlier version that ran on the control computer, was a Windows program.) The trip is documented in Memo AV01-031t, and the software is documented in Memo AV01-029t.

In February 01, we delivered several further upgrades to the algorithms and software. The day algorithm requires a background library of the clear sky red/blue ratios. Up until this time, we had been using the background from another site and instrument. As part of this contract, we wrote programs to enable extracting and processing this background data for these instruments, and we extracted the background and set up the day algorithm in the field to use these inputs. The day algorithm was also updated to include a horizon mask and occulter mask, to mask out regions that do not represent sky data. The new night algorithm was installed; this was an algorithm based on the contrast between the star and its background, and adapted specifically for the lighting distribution at the SOR site. The day algorithm processing is documented in Memos AV01-032t and 035t, and the software upgrades are documented in Memos AV01-033t and 34. This work is documented in Tech Note 265, and it completed Primary Task 1 in the SOW.

Primary Task 2: In January and February 01, we updated the Unit 13 and 14 software interface code, as documented in Memo AV01-030t, and integrated in the algorithm improvements made for the Unit 12 system, as documented in Memo AV01-034t. The control and processing software for these units was different from that for Unit 12, partly

because of differing sponsor requirements (connections to another system), and partly due to impacts of running different generations of operating systems. Unit 12 runs under Windows 95, and Units 13 and 14 run under Windows NT. The control code for Units 13 and 14 was developed as a script running under the V++ image processing package, because this was felt to be more efficient than converting to the new camera library required for Windows NT. This work is documented in Tech Note 265, and it completed Primary Task 2 in the SOW.

Primary Task 3 and 4: Continuing development of algorithms was required under Task 3 in the SOW, as well as in Optional Task 3 and Optional Task 9 in Section 4. In addition, Task 4 in the SOW requires the development of a stand-alone image processing program. Most of the work on the day algorithm in the early part of the contract was partially funded under the earlier contract, and is already documented in Technical Note 265. This includes adapting the algorithm to run in real time, extracting the constants for the SOR site, and extracting the clear sky background for the SOR site. In June 03, we prepared a detailed talk for SOR providing an overview of WSI systems, day and night algorithms.

To further develop the Day algorithm, we developed a stand-alone processing code (Task 4), documented in Memos AV04-038t and 039t, and several new utility programs developed to support the effort, as documented in Memo AV04-043t. We processed a fairly extensive data set from Oklahoma, partly with funding from another sponsor. This gave us the opportunity to evaluate an extensive data set, and determine the strengths and weaknesses of the algorithm. These results are documented in Memos AV04-047t, 049t, and 050t. The results were presented to the sponsor in talks in June 04 and November 04, and will be discussed in Section 7.

Some of the work on the night algorithm in the early part of the contract was partially funded under the earlier contract, and is already documented in Technical Note 265. This includes adapting the contrast-based algorithm for running in real time, updating it to work under moonlight, extracting the geometric calibrations, adding the ability to mask the horizon and occulter, and extracting the appropriate inputs for use at the SOR site. This work is documented in Memo AV03-030t. We also began work toward extracting beam transmittance for the night sky, and tested initial concepts for a full resolution night algorithm. This work will be discussed in Section 8.

Although both the day and night algorithm have continued to evolve, we believe that this work described above and further documented in Sections 7 and 8 completed the requirements of Primary Tasks 3 and 4.

Primary Task 5 is to provide a final written report, which is this report. In addition, interim verbal reports were provided via Power Point talks in June and December 2003; January, July and December 2004; April, June, August and December 2005; and February 2006. Much of the work in 2005 and 2006 was funded under the follow-on contract. Copies of these presentations are available to the sponsor on request. This report completes Primary Task 5.

Primary Task 6 in the SOW is to provide minor repairs as needed. This was for Unit 12, the WSI at SOR. As it turns out, Unit 12 was hit by lightning, and more major repairs were funded under the options, and are discussed below, as well as in Section 6. The work documented in Section 6 completes Primary Task 6.

Optional Tasks 1 and 2 given in Section 3 essentially allow work on options coordinated by MPL and SOR. These options are discussed in detail in Section 4, and become Optional Tasks 1 – 11 in Section 4. They will be discussed below. Optional Task 3 in Section 3 is to provide a final written report and interim verbal reports. The work is discussed in this final report, and was reported in the verbal interim reports documented two paragraphs above.

Optional Task 1 in Section 4 was to repair Unit 12, which had been hit by lightning. Problems were diagnosed and mostly repaired during a trip in October 03, and in cooperation with the sponsor during November 03, as documented in Memos AV03-049t and AV03-052t. Repair to the unit included replacing the photodiodes in the filter changer, replacing the DIO card, replacing the computer power supply, replacing a camera card, and repairing the flow system. This work completed Primary Task 6 as well as Optional Task 1 in Section 4.

Optional Task 2 in Section 4 was to deploy Unit 14 to Virginia. Earlier in '03 (and to some extent '02), we had supported the test of Unit 14, and its preparation for deployment. In November 03, we deployed the unit to Virginia. Memo AV03-047 documents the new control system software, and Memo AV03-048t documents the processing computer software. Memo AV03-054t is the trip report, and the components are given in Memo AV04-007t. This completed Optional Task 2 documented in Section 4. We also had some problems with this unit, and support memos AV03-055t and 56t and AV04-001t were provided to help support the field team. This work completed Optional Task 2 in Section 4.

Optional Task 3 in Section 4 was to continue the night transmittance map development work; this was discussed earlier in conjunction with the algorithm work, and will be further detailed in Section 8. This work completed Optional Task 3 in Section 4.

Optional Task 4 in Section 4 was to begin to evaluate optimal WSI designs for the future. As part of this work, we evaluated occulter redesigns. We had designed and built an occulter using an encoder under funding from another sponsor, but had not been happy with the encoder performance. We purchased a different encoder, and tests with this one were successful. We also evaluated current cameras available. We found that the Photometrics cameras are no longer available, but have been replaced by Princeton Instruments cameras. However, the latter company is not experienced with bonding of a fiber optic taper on the chip, so it may be necessary to redesign in the future to avoid this issue. However, the new cameras are air cooled, and that will simplify the environmental housing requirements. We did a pre-design for a “virtual ACP” that nearly eliminates the Accessory Control Panel, and presented these concepts at the December 2004 talk. Some

of this work was funded under the follow-on contract that started in September 04. This work completed Optional Task 4 in Section 4.

Optional Tasks 5 – 8 in Section 4 were all related to the Unit 14 support. A trolley repair was completed in April 04, and documented in Memos AV04-032t, 33t, and 34t. This completed Optional Task 5 in Section 4.

For Optional Task 6 in section 4, we calibrated both the fielded sensor and the repaired sensor. We first documented in Memo AV04-002t (January 2004) how to apply the calibrations that had been acquired earlier, in July 2000. The field calibration program originally developed for another sponsor was updated to work with the SOR systems, as documented in Memo AV04-030t. We evaluated some questions related to the impact of shutter timing, as documented in Memo AV04-024t, and then calibrated the Unit 13 camera system in May 2004, as documented in Memo AV04-025t and 27t. The camera housing was exchanged with that in the field in June 04, and documented in Memo AV04-035t. As part of this trip, we also repaired an environmental housing temperature sensor, and changed the GPS update interval to be compatible with the site constraints. The returned camera was also calibrated on return, and documented in Memo AV04-045t and 046t. This completed Optional Task 6 in Section 4.

For Optional Task 7 in Section 4, we built a glass dome with heater into the camera housing. This is designed to evaporate dew and snow on the dome in the winter. It was installed in the camera housing prior to the calibration discussed above, and installed in the field in June 04, as documented in Memo AV04-035t. During fielding we found it was better not to run it in the summer. This completed Optional Task 7 in Section 4.

For Optional Task 8 in section 4, we also updated the flux control to work for this very bright location. We analyzed the open hole data, as documented in Memo AV04-054t, and decided that we would like to evaluate data taken spectrally at this site. The flux control was updated to acquire spectral data at night, as documented in Memo AV04-035t. This completed Optional Task 8 in Section 4.

As noted earlier, Optional Task 9 was intended to be addressed primarily under the next contract, DO #11, but could be addressed under this contract also. A theoretical and practical analysis of the use of IR imagers in meeting the project needs was done, and the results presented in July 04. These results are discussed in Section 9. This work completed Optional Task 9 in Section 4.

As documented above we have, with the completion of this report, completed all contract requirements for Contract N00014-01-D-043 DO #4 to the best of our knowledge.

6. Discussion of Hardware Developments

As discussed in Section 5, during this interval we continued maintenance of the WSI Unit 12 at SOR, and also deployed WSI Unit 14 to Virginia. The Unit 12 system generally operated fairly well, although it required extensive repair following the lightning strike,

and somewhat more repairs than normal during the period after that. However, the in-house records show a high number of repairs required for Unit 14. The unit ran essentially flawlessly during a several month deployment to Northern California, and it ran essentially flawlessly during extensive test periods at MPL. We had several problems at the Virginia site. Some were, we believe, due to the inexperience of the personnel at the site, and some may have been because this was a new version of the instrument. The truth is that we cannot account for the relatively poor behavior of the instrument at the site.

Some additional memos related to general instrument repair that have not already been listed in Section 5 are memos AV01-068t, AV01-070t, AV01-080t, AV01-092t, AV03-048t, AV04-009t, AV04-011t, AV04-013t, AV04-026t, AV04-029t, AV04-031t, and AV04-044t. These memos, listed in the Reference section, document the instrument part numbers, return of the unit from Northern California, software upgrades, procedures for making repairs, check lists, and so on.

Work under Optional Task 4 of Section 4 to evaluate optimal WSI designs for the future was discussed in section 5. We would like to enlarge on two areas, the occulter modernization and the ACP modernization.

The normal occulter design with the trolley, shown in Fig. 1, obscures about 2.1% of the sky. However, we make the mask slightly larger than the actual occulter, because there is some uncertainty in the position. We find that a 1% uncertainty covers most occurrences. Because the rails and chains are close together, if there is a 1.0° uncertainty in occulter position, the resulting occulter mask covers about 9.1% of the sky. A new occulter was designed to address this, under funding from another program. It is not only smaller, but also has a more accurate readout on position, so that a 0.5 to 1° tolerance can be used. This is shown in Figure 2. This results in a 4.6 – 5.5% loss over the sky, as opposed to the earlier 9.1% loss.

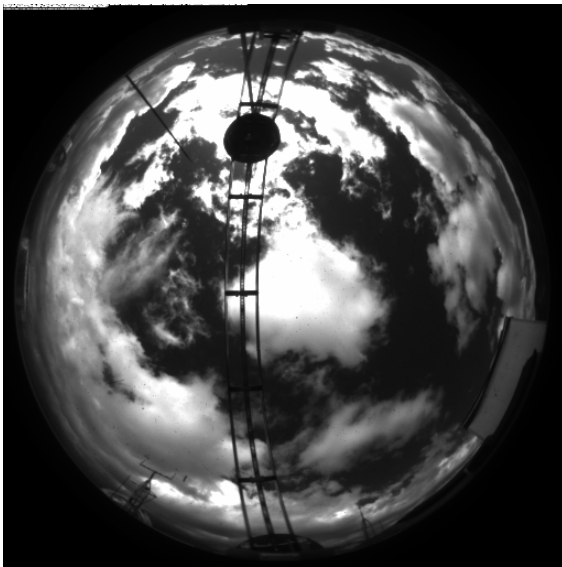


Fig. 1. Profile of standard WSI occulter

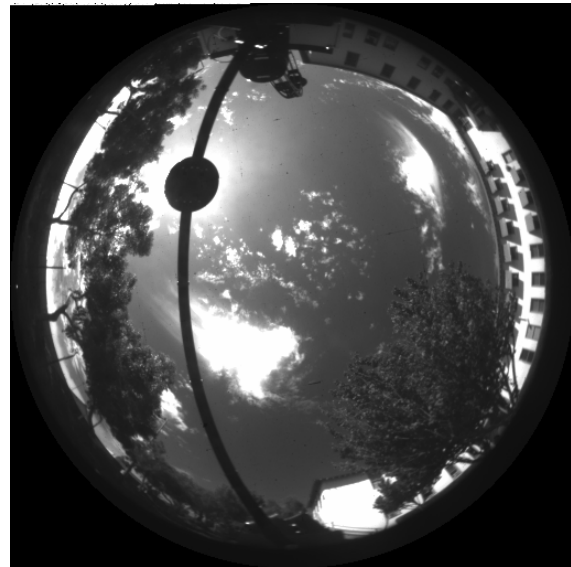


Fig. 2. Profile of Improved Occulter

In order to improve the position accuracy, this occulter is less mechanically flexible, and it also uses absolute encoders to provide a more accurate readout. Also, it will be less costly to build, as it does not require as much control electronics fabricated at MPL.

Unfortunately, at the time the occulter was designed, only one company provided an encoder that met the necessary specifications, and this encoder turned out to have reliability issues. Since that time, a similar encoder became available that was manufactured by a more well-known company, and that also met the required specifications. Under the SOR contract DO #4, we purchased one of these encoders and its software and tested it, and found that it was both reliable and compatible with the WSI system. In the future, if more WSI systems are built, we would recommend using this new encoder with the new occulter design, unless a better occulter is designed in the interim.

Another significant upgrade we evaluated is simplification of the Accessory Control Panels. These ACP's control the occulter shown in Fig 1 and the filter changer, and they provide readout of the various environmental housing protection sensors, such as the flow sensor and the temperature sensors. They enable the system to be run either manually using switches, or with computer control. At this time, we feel that the manual interaction is not required, and a much simpler ACP can be designed. Preliminary concepts were developed under this contract, and tested under the next contract. A preliminary design of the interface, which would now be a computer interface rather than a panel with meters, is shown in Fig. 3. This upgrade should both lower cost and increase reliability.

7. Day Algorithm Developments and Analysis

As discussed in Section 5, during the early part of this contract, much of the work on the day algorithm involved upgrading the SOR site. We had a day cloud algorithm that could be run in the field, however it was running on the same computer as the data acquisition, and did not allow the system to be run at 1-minute intervals. We added a processing computer, and adapted both the control and the processing logic for this setup. We also installed a NIR filter, which should do a better job with thin clouds under hazy conditions, and adapted the programs to handle this data acquisition.

The clear sky background is a necessary part of the thin cloud part of the cloud algorithm, and fairly time consuming to extract from the field data. Up until this time, we had used the background extracted for another site, and told the sponsor that the thin cloud results should not be considered valid. As required under Primary Task 1, we extracted the clear sky background for SOR, along with the other parameters that are required to run the algorithm, thus providing SOR with thin cloud results.

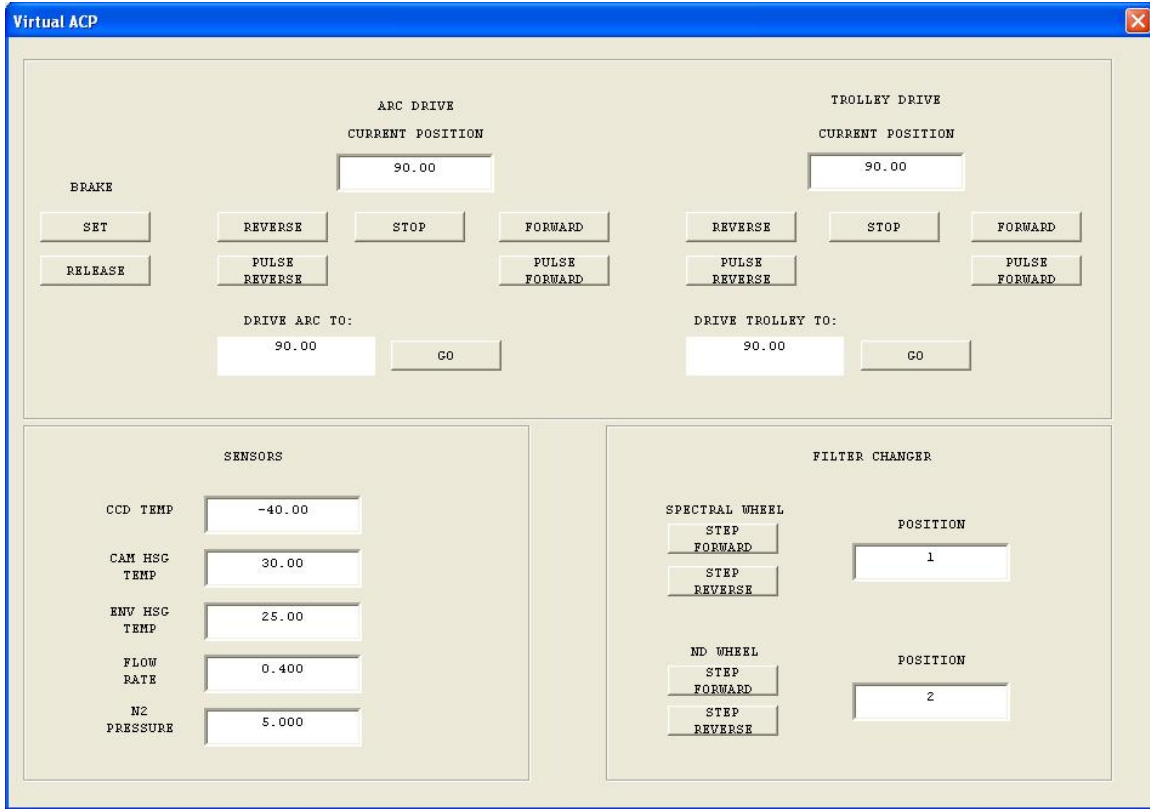


Fig. 3. Initial design for computer control to replace Accessory Control Panels

Under this contract, we then developed a stand-alone day algorithm program for use at MPL in testing the strengths and weaknesses of the algorithm, as we had not had the opportunity to evaluate an extensive data set to see how well the algorithm performed. Also, support programs, documented in Memo AV04-043t, were developed to make the processing somewhat more efficient. We were funded by another sponsor to process data from an Oklahoma site for a full two months and portions of several other months were processed, in order to extract Cloud Free Line of Sight (CFLOS) (Shields et al. 2005b). This provided the most efficient mechanism for us to evaluate the general strengths and weaknesses of the algorithm for the SOR program, since the data was already processed, and the site was midway in haze level between the SOR and the Virginia sites.

In general, we were quite pleased with the results. Sample results are shown for February in Figures 4 and 5, and for August in Figures 6 and 7. In these figures, dark blue represents regions identified by the algorithm as clear, light blue represents thin cloud, and white represents opaque cloud. Black pixels represent “no data”. Note that the horizon mask is higher in the August data, because the prairie grass had grown up into the field of view.

Normally the two most difficult regions for a cloud algorithm are the horizon and the solar aureole. The algorithm generally handled these regions quite well. Especially in Figure 5, it is easy to see that the cloud discrimination near the horizon is excellent. Similarly, the bias with solar scattering angle is very small, as can be seen particularly in

Figure 7. That is, the cirrus are identified quite well near the sun as well as at angles well away from the sun.

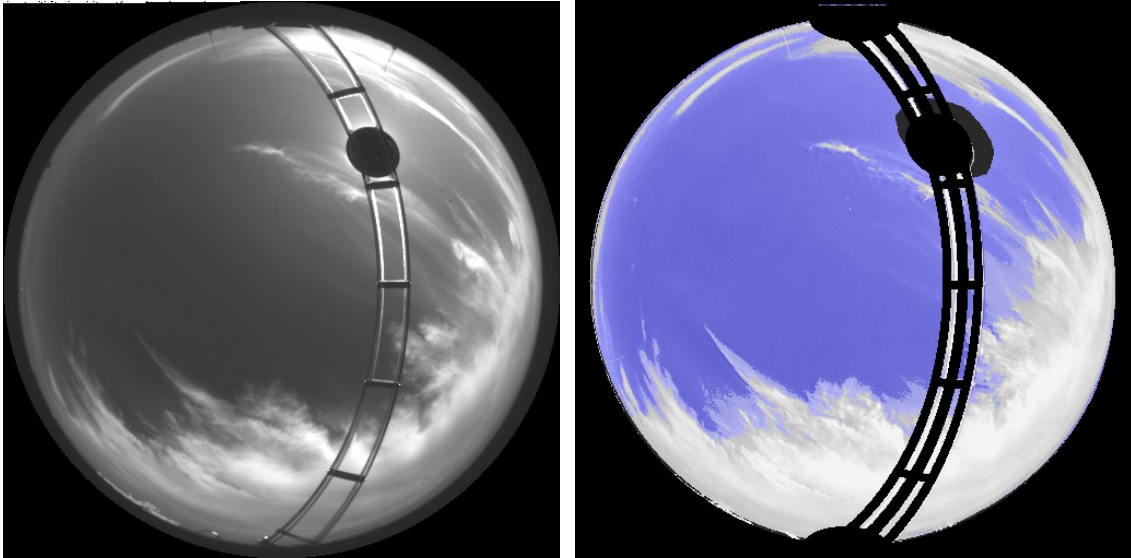


Fig. 4. Raw Red and Processed Cloud Decision for 20 Feb 02,1420 GMT.

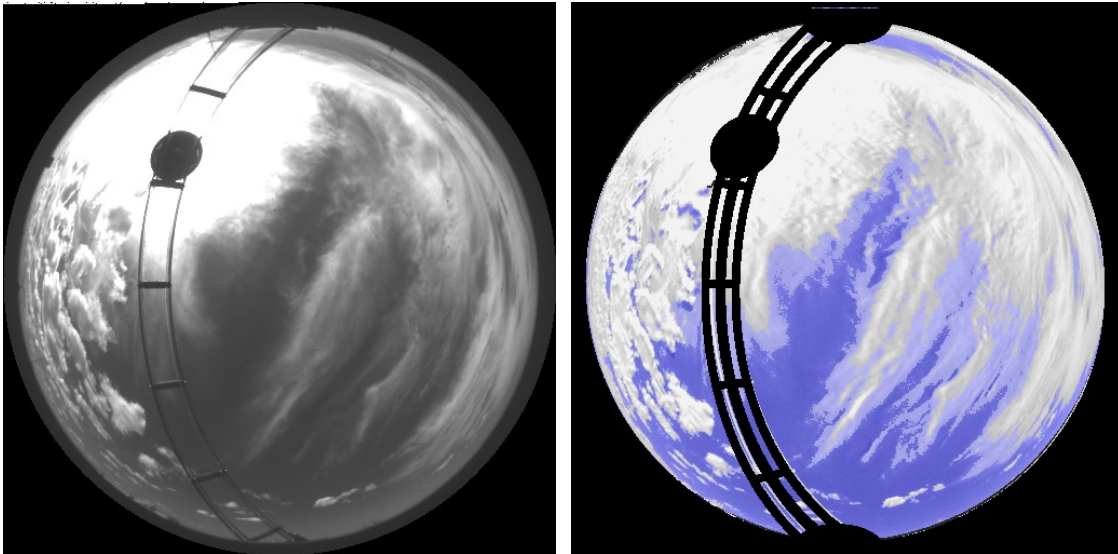


Fig. 5. Raw Red and Processed Cloud Decision for 21 Feb 02, 1700 GMT.

In our evaluation, we found that there were two primary problem areas with the algorithm. First, we found that about a third of the time, the results were not valid for sunrise and sunset. This is a difficult time regime that will require some work. Second, the algorithm does not yet handle haze optimally. Examples are shown in Figures 8 and 9. In the February data, we did not lose any data due to haze, but we lost nearly a third of the August data due to haze.

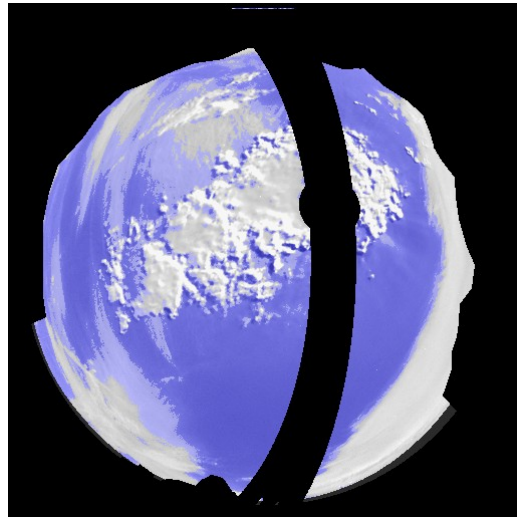
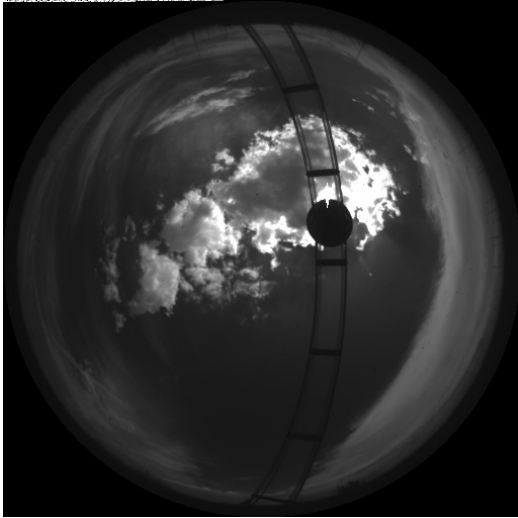


Fig. 6. Raw red and Processed Cloud Decision for 12 Aug 02, 1706 GMT.

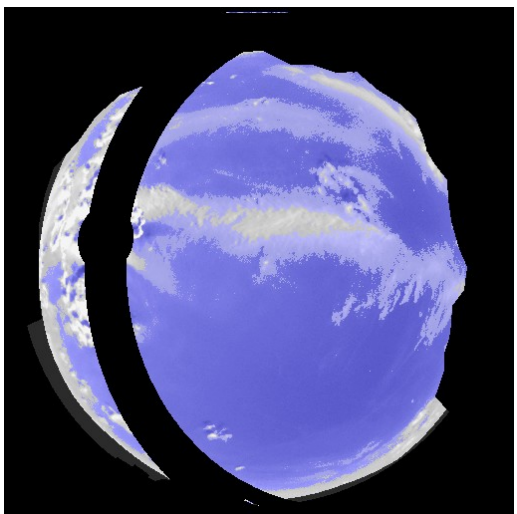
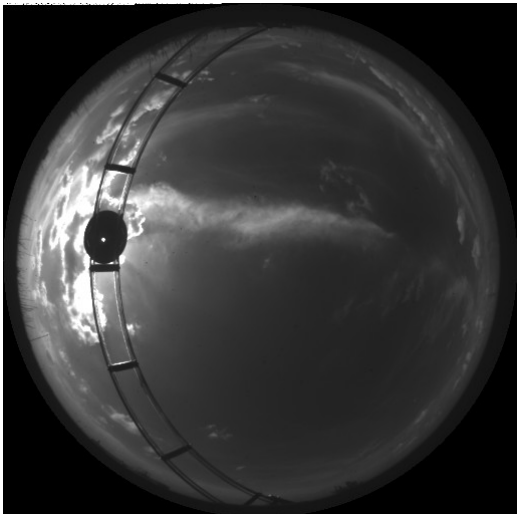


Fig. 7. Raw red and Processed Cloud Decision for 16 Aug 02, 2200 GMT.

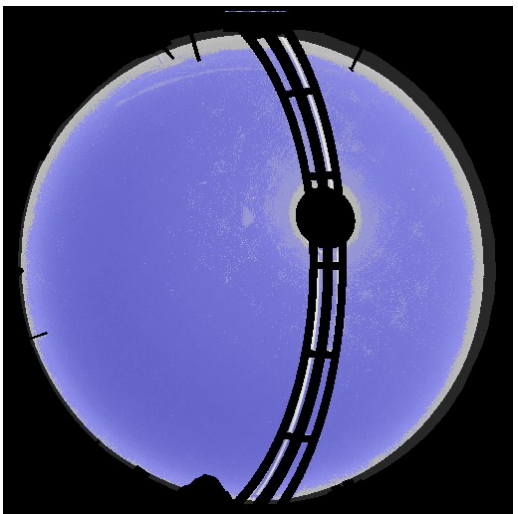


Fig. 8. Forward bias haze case

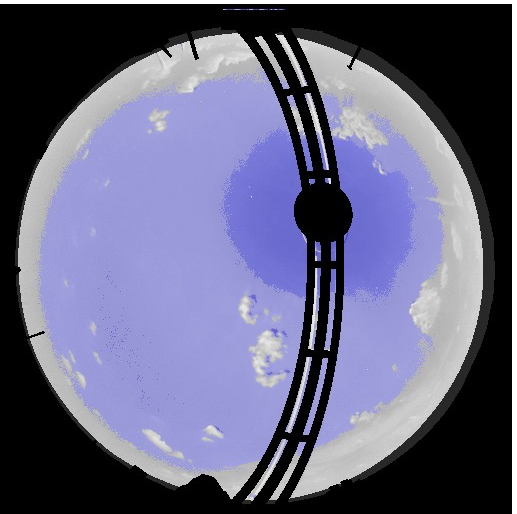


Fig. 9. Reverse bias haze case

During this period, we were funded to develop a better haze algorithm for the Day WSI (Shields et al. 2003d). As documented in Memo AV04-014t, we were able to significantly improve results for the Day WSI by making two changes. The new Day WSI algorithm uses NIR/blue ratios in place of red/blue ratios, and it also adjusts each image for the current haze amount. Similar upgrades have been partially completed for the Day/Night WSI under the follow-on funding, and are anticipated to be the next major improvement in the day algorithm

Although we feel that the developments made on the Day WSI should address the issue with haze for most conditions, there was another really interesting thing about the haze cases from August. Although generally the haze caused a false call of thin cloud near the aureole, as shown in Fig. 8, some resulted in a false call of thin cloud everywhere but the aureole, as shown in Fig. 9. We have not yet seen this occur elsewhere. The identification of a thin cloud depends on the current red/blue ratio, in comparison with the nominal clear sky ratio. When we were first developing the cloud algorithm, in the mid 1980's, we found that in general, the shape of the clear sky ratio distribution is reasonably fixed, as a function of scattering angle and look angle, even in varying haze amounts. However, in Figures 8 and 9, the ratio near the aureole is varying in comparison with the rest of the sky, as shown in Figures 10 through 12. We would anticipate that this is due to a change in the drop size distribution, which affects the aureole most strongly. If this turns out to be a common occurrence, then we will need to make the algorithm more sophisticated to handle this.

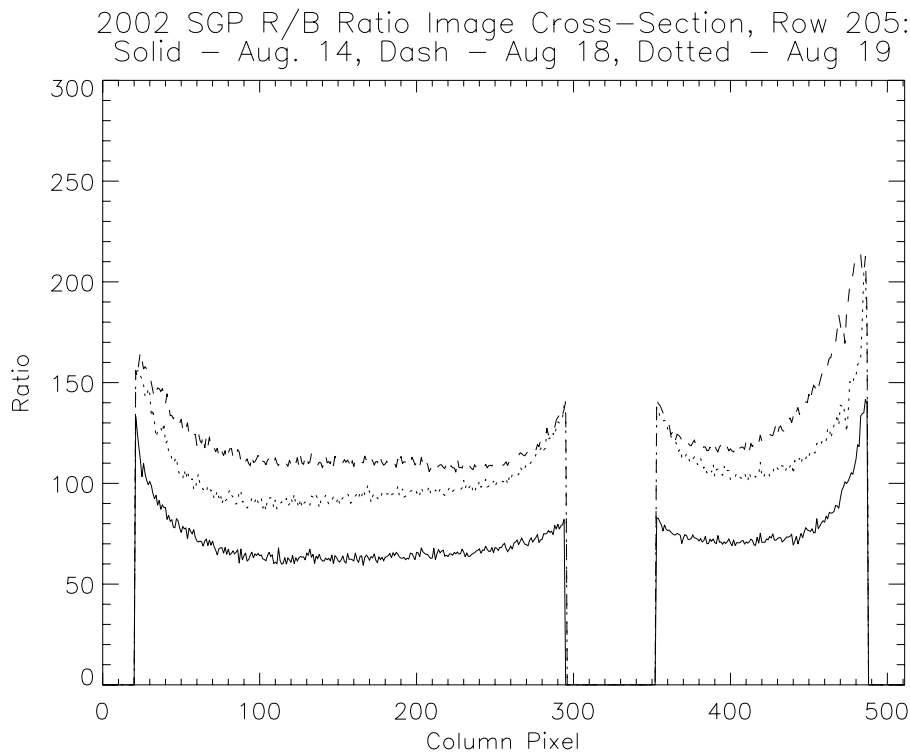


Fig. 10. Red/blue ratio in a column through the sun on 3 typical days.

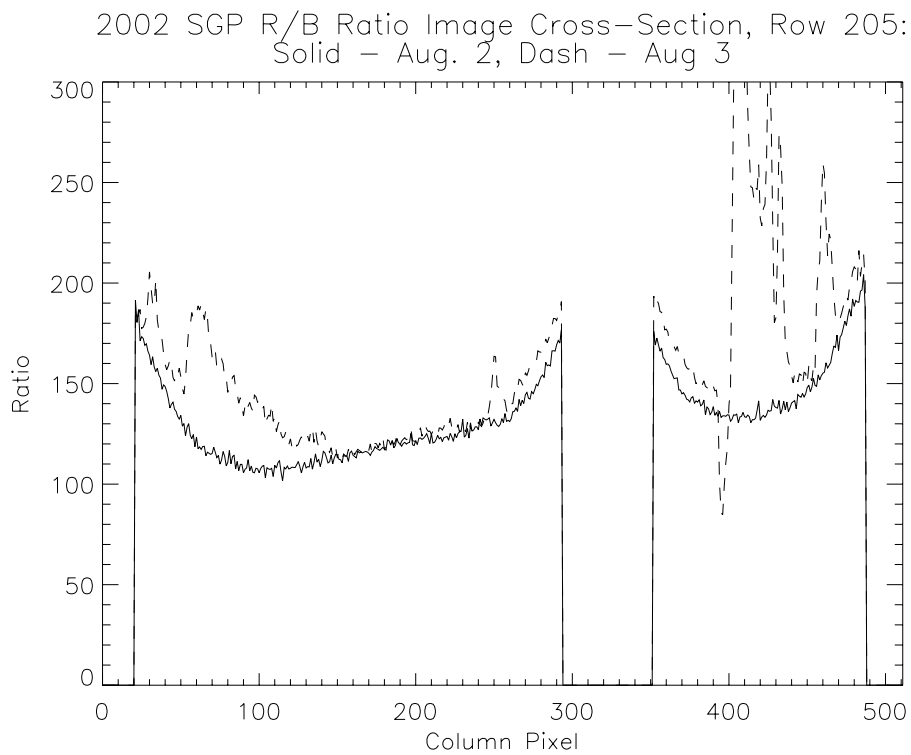


Fig. 11. Red/blue ratio in a column through the sun on 3 days with enhanced aureole ratios or forward bias.

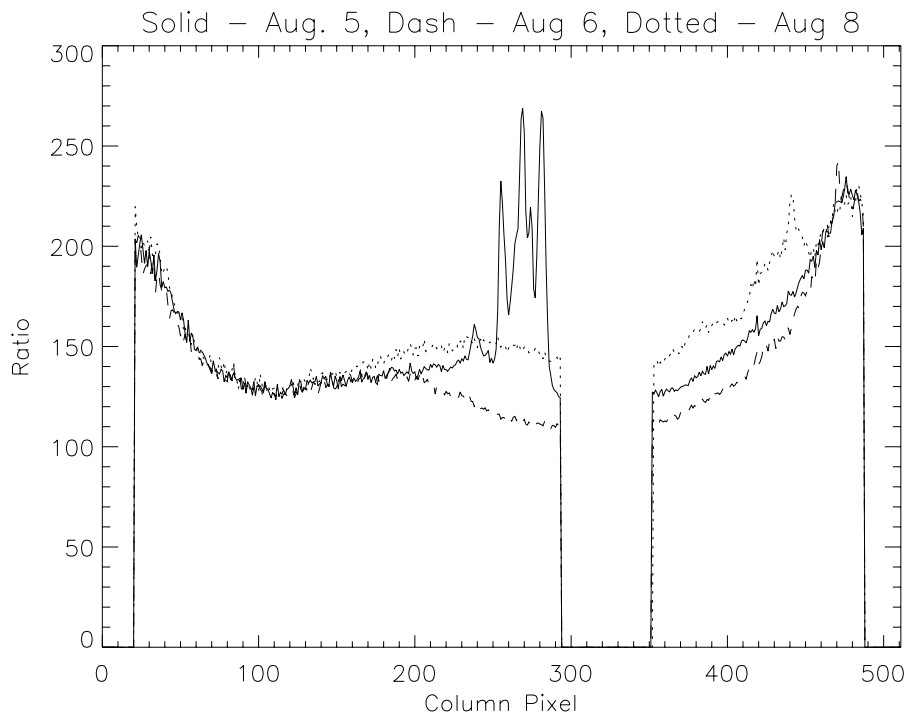


Fig. 12. Red/blue ratio in a column through the sun on 3 days with low aureole ratios, resulting in reverse cloud bias.

In addition, we hope in the future to extract aerosol information from the WSI. We see the red/blue and NIR/blue ratios vary with the amount of haze. Variations in the radiance across the sky, particularly near the aureole, may also become useful in extracting other information related to the aerosol.

In short, the day algorithm work done under this contract enabled us to get a real time day algorithm optimized for SOR with the correct clear sky background, and then we developed a stand-alone version of the code for analysis of data at MPL. As a result, we were able to evaluate an extensive data set, and determine the strengths and weaknesses of the algorithm. Much of this work was presented in a talk at SOR in December 2004.

8. Night Algorithm Developments and Analysis

To identify the presence of clouds at night, it is first necessary to detect them, i.e. to have raw data in which the clouds may be distinguished. Since often the assumption is made that this is impossible with a visible system, we would first like to note that we have not yet seen a situation in which the clouds are not clearly visible in the imagery – even when they are not visible to the human eye. As an illustration, Figure 13 shows a moonless night from a site with minimal lights in the surround. Figures 14 and 15 show a moonless night from a site near a city. The system has a grey scale of 0 to 65,535, with a readout noise near 1. As a result, it is difficult to show the full range in an illustration. Figure 14 has been windowed to show the clouds in the darker part of the sky, and Figure 15 has been windowed to show the clouds in the brighter part of the sky. Figure 16 shows a moonlight image. In all cases, the data is clearly present for detecting the clouds.

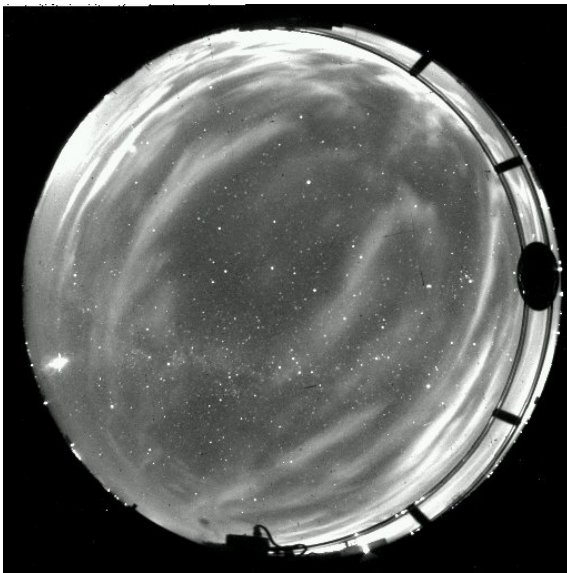


Fig. 13. No moon case in Oklahoma, File 73520120

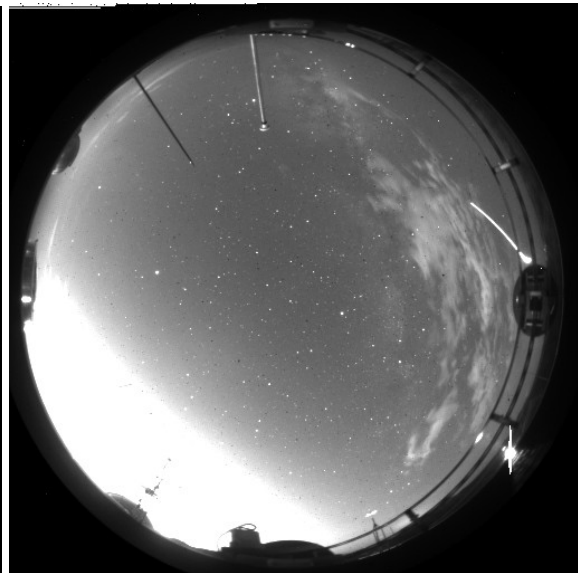


Fig. 14. No moon case, SOR, enhanced to show clouds away from city

Our first version of the night cloud algorithm was programmed for the SOR site just before this contract started, and reported in Shields et al. 2004b. This is a moderate

resolution algorithm, based on contrast between the sky and background. It is still in use at some WSI sites, and will be referred to as the contrast-based algorithm. Examples of results are shown in Figures 17 – 19. This version of the algorithm required quite a bit of development, as we had not previously handled moonlight, nor did we previously have an automated algorithm. We were reasonably pleased with the results.

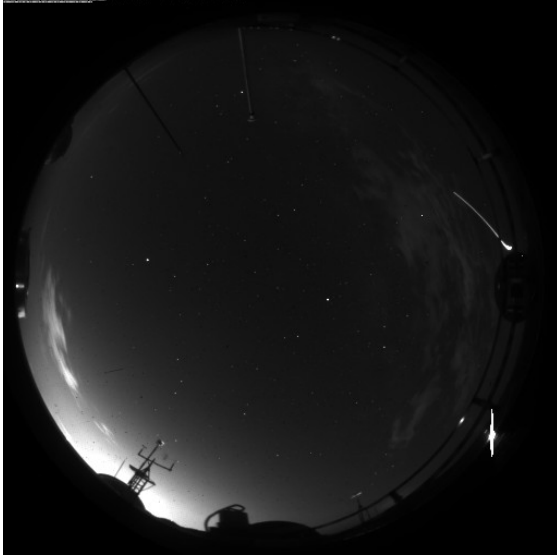


Fig. 15. No moon case, SOR, enhanced to show clouds near city

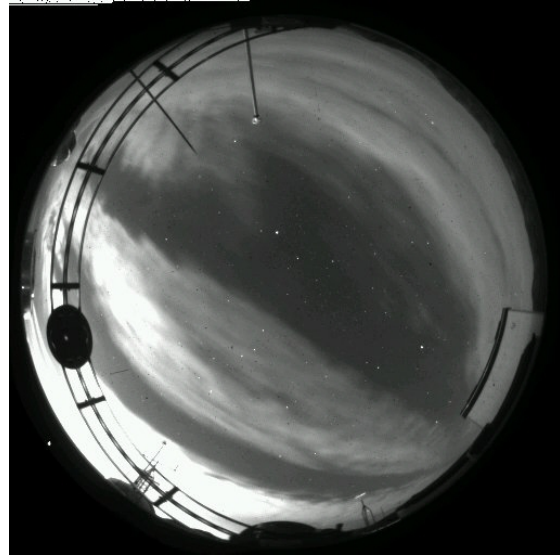


Fig. 16. Moonlight example

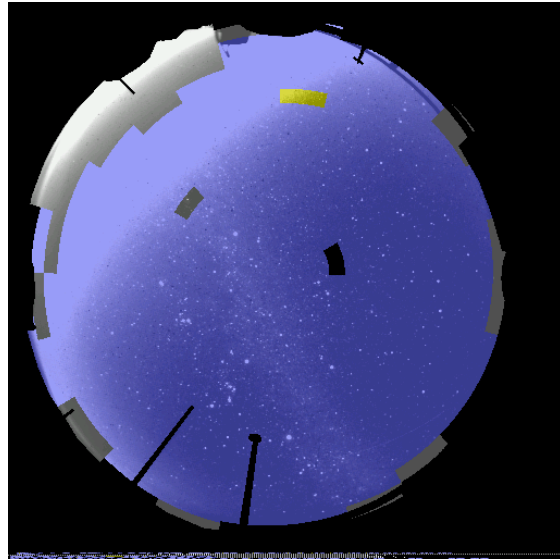
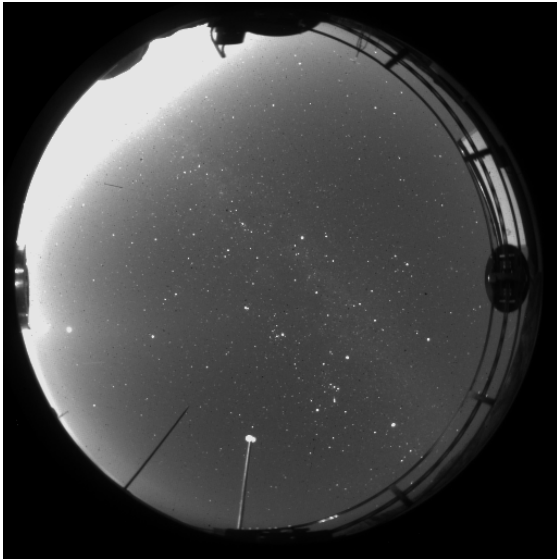


Fig. 17. Night raw and processed data for a clear case (N/S reversed in these images)

This contrast-based night algorithm is based in part on the detection of approximately 2000 stars per image. An angular calibration using star position was developed, to provide accuracy to within about $\frac{1}{2}$ pixel or $1/6^\circ$. Decisions are made within each roughly 5° zenith by 15° azimuthal cell. For more details, see Shields et al. 2004b.

Although the algorithm worked reasonably well, it did not handle the city lights well, and we wanted to develop, in the long run, a full resolution algorithm, i.e. one that makes a decision at each pixel, as the day algorithm does.

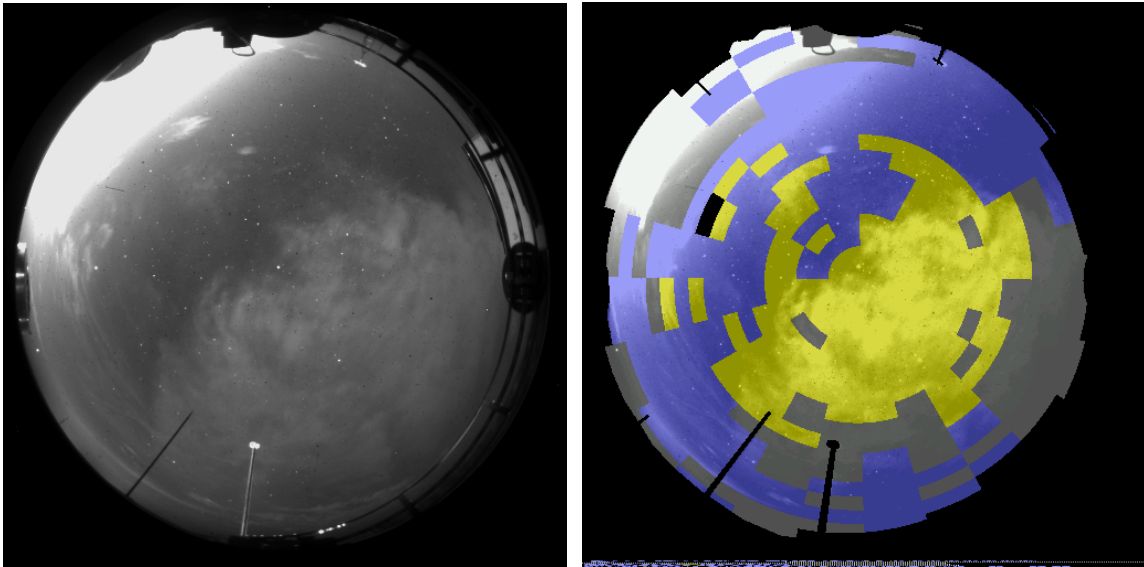


Fig. 18. Night Raw and processed data for a broken cloud case (N/S reversed in these images, yellow is thin cloud)

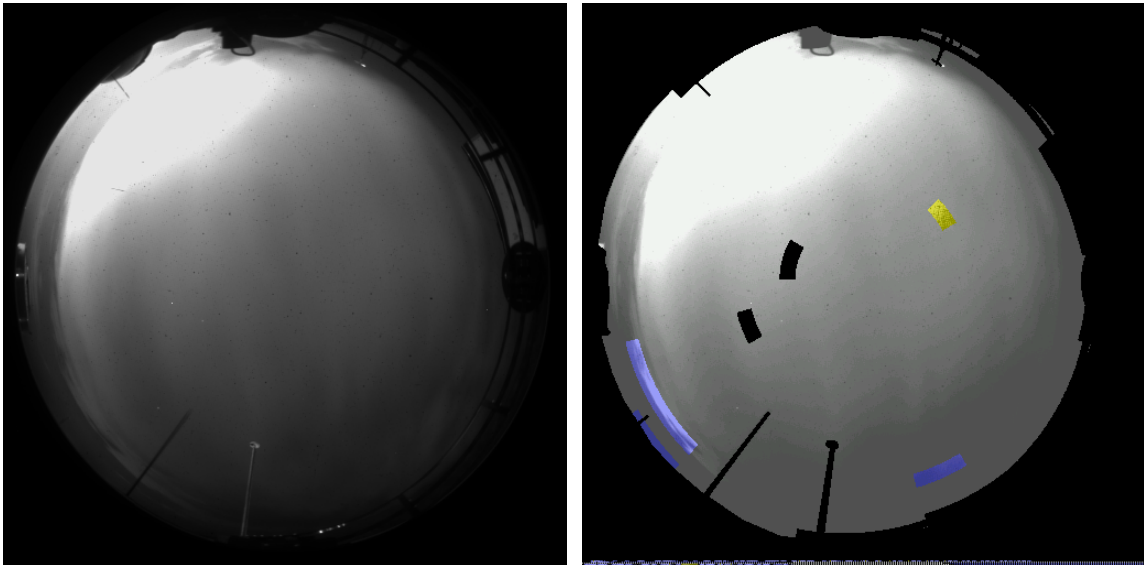


Fig. 19. Night Raw and processed data for an overcast case (N/S reversed in these images)

Under Delivery Order #4 (the contract being discussed in this report), we developed the first concepts for a full resolution algorithm, as documented in Memo AV01-069t. The first step required in order to develop the full resolution algorithm is to calibrate the images for absolute radiance, and then extract the earth-to-space beam transmittance for selected stars. All 3 of the SOR units were calibrated, as documented in Memos AV01-041t through AV01-067t and AV01-094t. Software was written to apply these calibration results to field images, as documented in Memo AV03-037t.

As noted in Section 5, later in the contract we were given the field calibration device we had developed for another sponsor, and we adapted the software to work with the SOR Windows systems, as documented in Memo AV04-030t. This made the recalibration of Units 13 and 14 much more efficient (Memos AV04-024t, 025t, 027t, 045t, and 046t).

The next step required development of techniques to extract earth-to-space beam transmittance. We already had techniques to detect the stars, documented earlier. This transmittance work was heavily leveraged by funding from another sponsor, as reported in Shields et al. 2004a, Memo AV01-097t, and AV04-004t. As part of this work, we developed the equations for computing the inherent star irradiance in the WSI passband, based on the star library star magnitude and color temperature. We also developed techniques for determining the measured star irradiance from the calibrated radiance image. Figure 20 shows the results for the theoretical star irradiance, in comparison with measured star radiance, for approximately 1500 bright stars down to an irradiance of 10^{-9} watt/m²-μm (down to a star magnitude between 3 and 4, depending on color temperature). When stars to magnitude 6 are included, the results are reasonable, although more scattered, with a R² correlation value of .85 for 32,000 stars. In later work, to be reported in the next report, we were able to improve these results significantly, to yield a R² correlation value of .935 from the same site.

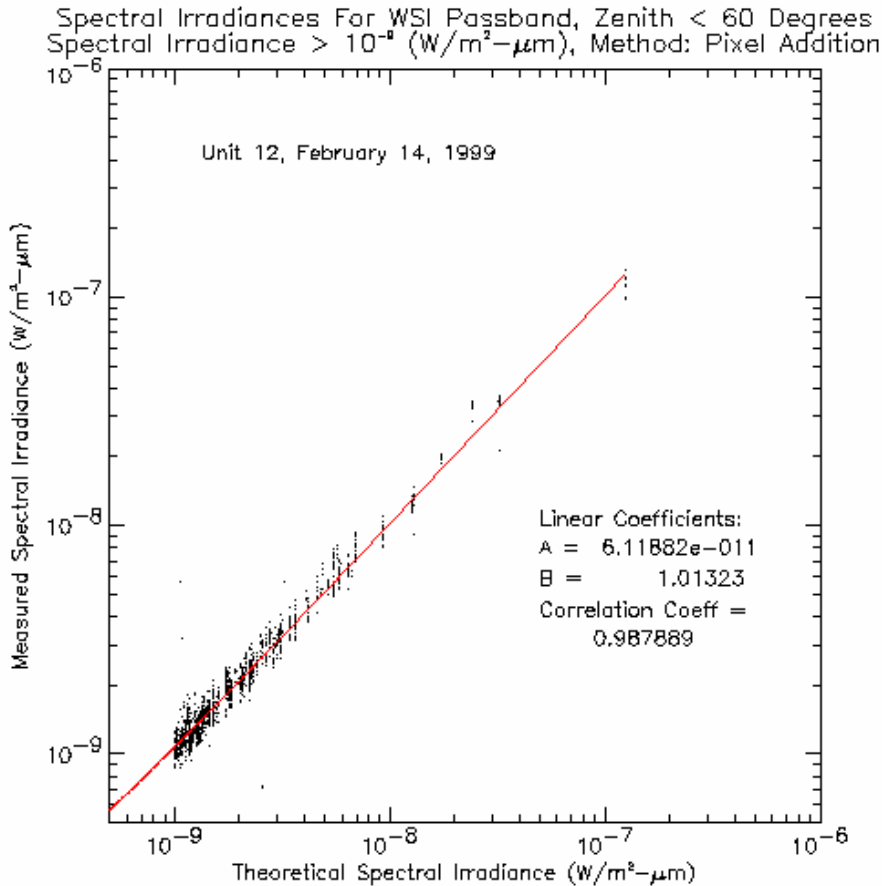


Fig. 20. Comparison of measured star irradiance, as determined from the calibrated radiance image, with the theoretical star irradiance, as determined for the WSI passband from the star library magnitude and color temperature.

An example of the resulting cloud transmittance map is shown in Figure 21. This has been generated by correcting the raw transmittance map with an aerosol transmittance of 0.8. The resulting ranges, less than .6 for cloud, and greater than .6 for the sky, seem very reasonable, although there is more scatter in the values in the clear regions than we would like.

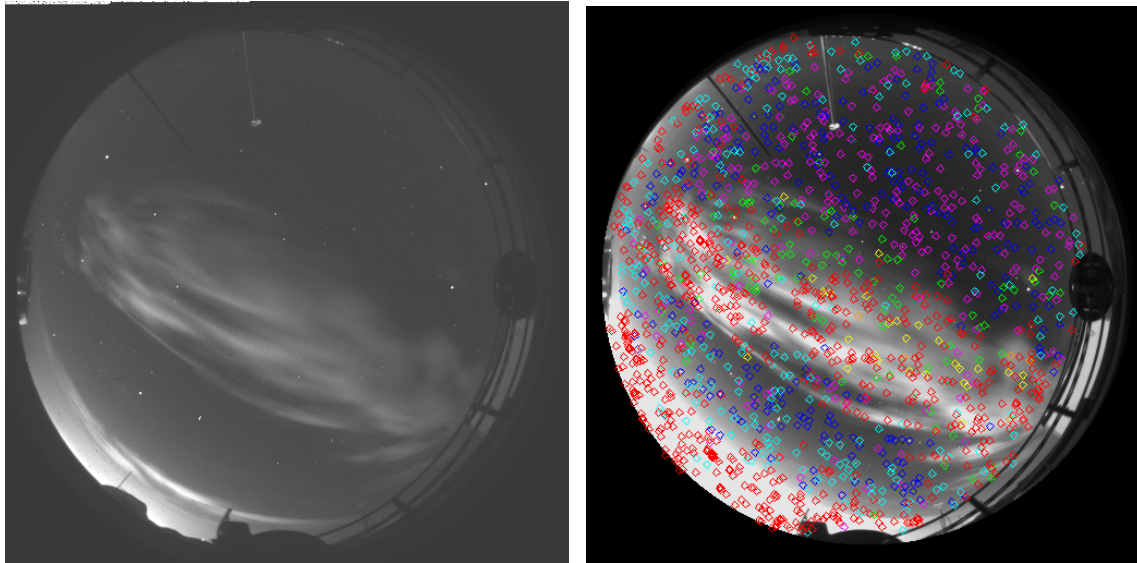


Fig. 21. Sample cloud transmittance extraction result. Color key: Red: no star detected; orange, yellow, and green correspond to transmittance ranges of 0 - .2, .2 - .4, and .4 - .6 respectively; purple, blue and turquoise correspond to .6 - .8, .8 - 1.0, and > 1.0 respectively

Additional work toward improved transmittances, a transmittance-based algorithm, a high resolution algorithm, and methods for ground-truthing the results, were continued under the next contract, and will be discussed in the next report.

9. Discussion of Wavelength Options for Optical Cloud Imaging

The sponsors would like to have the ability to detect clouds over the whole sky that will be of importance in attenuating transmission at or near $1.6 \mu\text{m}$ in the SWIR. Based on scattering theory, we would anticipate that a visible sensor like the WSI should do very well at this task. Clouds are typified by large droplets, in the regime of about $2 - 20 \mu\text{m}$ (Hobbs and Deepak 1981, see article by Cox, Fig. 1). Because the droplets are larger than the wavelengths of interest, the scattering losses should be similar for the visible and the SWIR. We also expect the scattering to be similar for the visible and the SWIR for light fog and heavy fog (Holst, 2000 Figure 5.7). Based on models H, L and M (McCartney 1976 Figure 3.8), haze tends to have drop sizes shorter than the $1 \mu\text{m}$. (Also see Hobbs and Deepak 1981, article by Jiusto Fig. 9, for an example of haze developing into fog.) Thus we expect that the scattering losses in the SWIR will be less than those in the visible.

As a result, the WSI should detect all scattering losses of importance in the SWIR. The WSI will also detect the haze, and it will be important that the haze not be identified as

cloud. However, it will be useful if the WSI algorithms identify cases with heavy haze that might affect the SWIR. We should also note that although we have not extensively evaluated the absorption, we would expect that absorption losses should not be significant in the SWIR, except for ice near $1.61\ \mu\text{m}$.

Although we feel the WSI should do an outstanding job detecting the scattering losses that impact the SWIR, we and our sponsors felt that this question was worth further evaluation. Under this contract, we made a preliminary, but fairly extensive, evaluation of the pros and cons of using sensors in the visible, in the short wave infrared (SWIR) at $1.6\ \mu\text{m}$, and in thermal infrared (IR) wavelengths for this purpose. The analysis was presented in a talk on July 04. The Power Point file can be provided to the sponsors upon request. In Section 9.1 below we discuss an experiment to evaluate how well SWIR sensors can perform for this task. This experiment also evaluated how well the visible sensor detects the clouds seen in the SWIR. In Section 9.2 we provide a general evaluation of available imagery from IR cloud detection systems. In Section 9.3, we briefly evaluate Mid Wave IR. In Section 9.4, we provide a theoretical analysis of the Long Wave IR potential for our applications.

The Power Point talk also included a general overview of the theory, including plots of the drop sizes associated with haze and with clouds, and the impacts of scattering and extinction in the different bands. This is not included in this report, as it is already covered in numerous theoretical texts.

Before we proceed further with the wavelength discussion, I would like to include one comment made during the talk, regarding the bias of our group. I have to admit that we love the WSI. We have found it to be a very capable and flexible instrument, and we have found that very good algorithms can be developed if the analyst is familiar with both atmospheric physics and the instrument performance and calibration characteristics. Some desired aspects of the algorithms are not yet developed, and also nothing is ever perfect. We have some experience with the IR and would love to gain more experience. It is in the University's interest for us to present a fair and unbiased evaluation, and that is what we will try to do.

9.1. The Visible and SWIR Intercomparison Experiment

If a whole sky imager could be developed that worked day and night, down to the horizon, directly in the SWIR wavelengths, this could have an advantage, because we would be measuring the clouds directly in the wavelengths of interest. During 2002 - 2004, under funding from another sponsor, we developed a SWIR calibrated fisheye imager, for use in an aircraft or UAV, looking down at cloud tops (Shields et al., 2003c).

While the system was still at MPL, we ran an experiment to compare the visible and SWIR systems looking up from the ground. One of the purposes of this experiment was to determine whether the WSI system is able to detect all of the clouds of significance in the SWIR wavelengths. A second purpose was to evaluate the effectiveness of the SWIR imager in measuring the clouds from the ground.

Several examples of image sets are shown in Figures 22 through 25. The images were not exactly simultaneous, because we had only one solar occulter. We acquired an image with one camera, moved the occulter, and then acquired the image with the other camera, obtaining images within about a minute. In each image, the SWIR image is shown on the left, and the visible image is shown on the right.

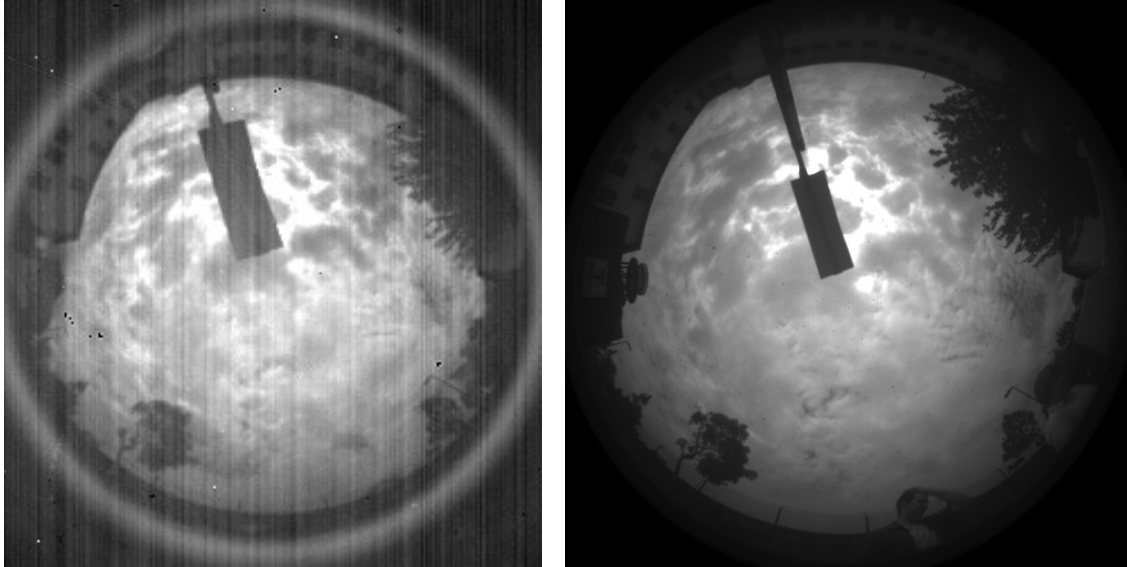


Fig. 22. Overcast case, imagery at 1.6 μm and at 650 nm 7 May 04 near 1040 Local

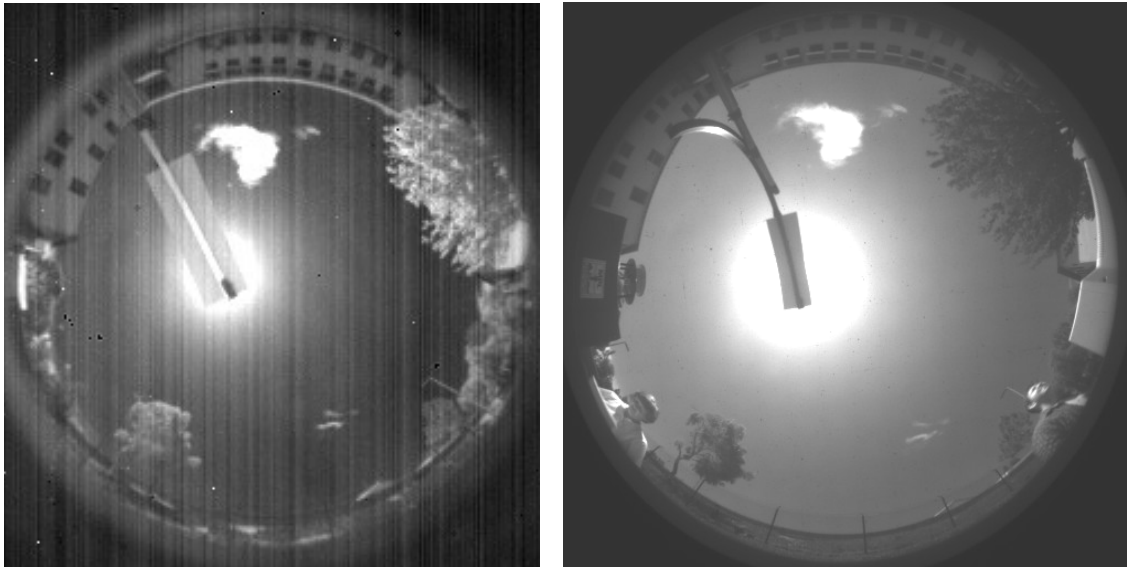


Fig. 23. Thin clouds, imagery at 1.6 μm and at 650 nm 7 May 04 near 1230 Local

In Figure 22, we had an overcast of fairly heavy clouds, and the images are quite similar in terms of the clouds detected. The quality of the raw data is superior in the visible, due to the camera technology (note the vertical lines and poorer resolution in the SWIR imagery on the left side).

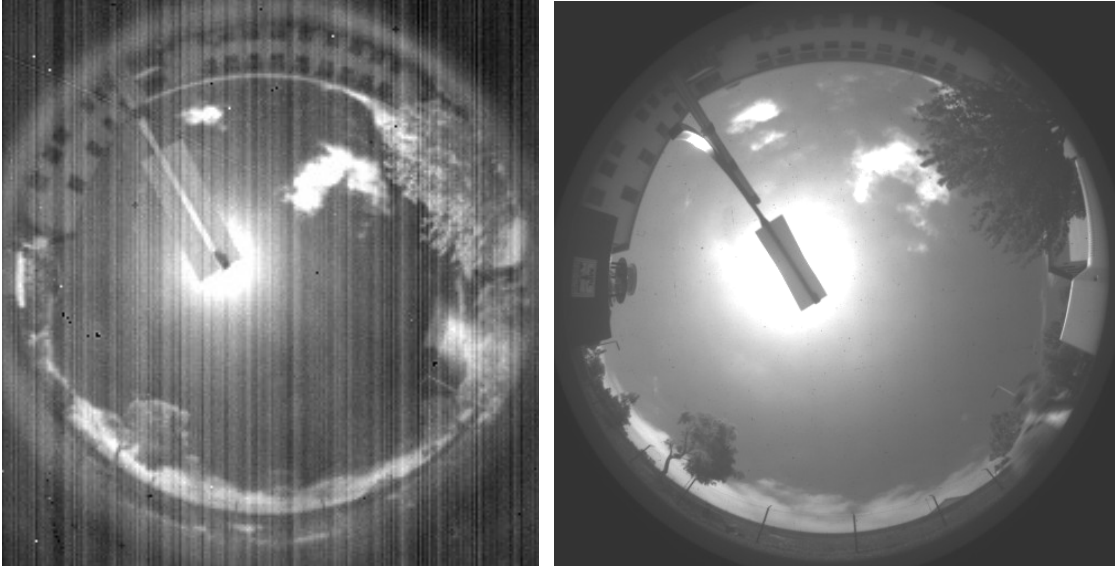


Fig. 24. Thin and pre-emergent clouds, at 1.6 μm and at 650 nm 7 May 04 near 1221 L

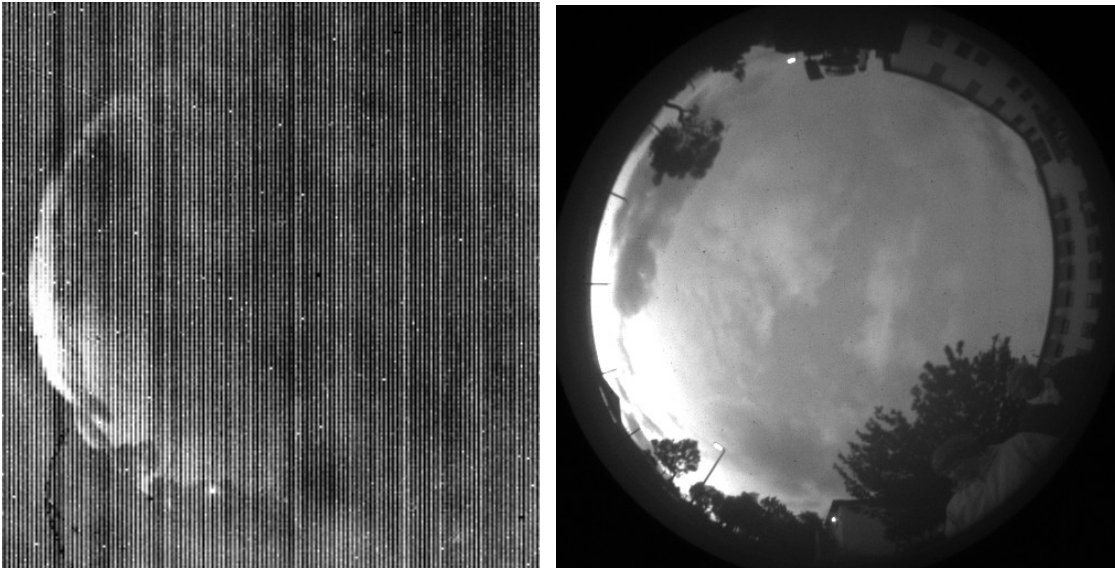


Fig. 25. Sunset, images at 1.6 μm and at 650 nm 11 May 04 near 1942 L

Relatively thin clouds are shown in Figures 23 and 24, and Figure 24 also included pre-emergent clouds. In this situation, the haze is beginning to acquire texture and become slightly more white, and clouds are about to form. This is less obvious when seen visually (with a human Photopic peak response near 555 nm), because the WSI image is at 650 nm, where the spectral contrast between the background haze and the larger droplets is increased over the visible. We do not yet know if it will be important to identify these as clouds for SWIR applications, but at least in this situation they were not seen in the SWIR image. From this imagery, it appears that the visible system detected all of the clouds seen in the SWIR.

There are two primary reasons that we feel a visible system will be superior to a SWIR system for the application of detecting significant losses in the SWIR transmittance.

First, the visible sensors are significantly superior, in terms of noise, uniformity, and linearity. We have calibrated both sensors very carefully, and for example at a signal of about 200, the SWIR system has a non-linearity error close to a factor of 1.8 (80% error). Secondly, the SWIR system has much less dynamic range than the visible camera used in the WSI, due to higher noise and limited grey scale range. Figure 25 shows an image near sunset, where the SWIR image is not very useful. The SWIR system was using a filter with a 50 nm passband filter. If this filter were removed, the sensor would see 2 logs (a factor of 100) darker. However, night imaging requires at least sensitivity 5 logs darker than the example shown in Figure 25. The WSI has a sensitivity that goes 7 logs darker than the setting shown in Figure 25. For these reasons, we do not recommend using a system at 1.6 μm at this time.

9.2. Thermal IR Systems

By making contacts with colleagues, and exploring the Internet, we were able to obtain information and/or sample imagery from three IR ground-based sky imaging systems with reasonably wide fields of view. These systems all are based on the Long Wave IR (LWIR) between 8 and 12 μm . These systems included: a) a system using an 18" mirror and a Raytheon 300A Uncooled Ferroelectric camera at 10 μm ; b) a system using a 150° lens and a New-Technology Uncooled Microbolometer operating at 8 – 13 μm ; c) a system with a 180° lens and an uncooled microbolometer. As part of this study, we also researched the available cameras from the IR manufacturers and evaluated their characteristics for the purpose of detecting the clouds; however this is beyond the scope we wish to include in this report.

Although we found several images on the web, we are in an awkward position, because we are no longer able to find the web sites in order to determine whether the images may be used in a formal document. In fact, one of the web sites disappeared shortly after we extracted the images. We know that at least one of these instruments is still in use at the current time, but we are not aware of images that are available for use in a report. At the time of the July 04 presentation, we tried to contact the source of the images we evaluated, and did not receive any response. As a result, we feel it is best if we do not include the IR images in this report, but simply report on our findings.

The IR images we observed have much lower resolution and appear to have poorer focus than the WSI. Also, the dynamic range of the cameras appears to be less than the dynamic range of the sky. That is, either the clouds or the sky are offscale, which would make algorithm development (if required) difficult. On the positive side, we found that the IR systems did not require a solar occulter, due to the relatively low brightness of the sun at these wavelengths. This makes sense, since from Holst 2000 Table 6-1; the solar radiation at ground level is only about 1.5 W/m^2 , whereas the self-emission of a 290° K target is 127 W/m^2 in the LWIR.

Regarding the dynamic range, the low opaque clouds appeared in the IR imagery to be not only brighter than the background, but also offscale bright. We did not find any examples of cirrus clouds detected by wide field of view IR imagers. In later searching,

we have found one example with cirrus clouds in the simultaneous visible image, and the IR detector does not appear to have detected them.

We did not find any imagers with a cloud algorithm, beyond a simple threshold that is tweaked from day to day depending on the haze level. If some of the clouds are offscale bright, as they appear to be, and some of the sky is offscale dark, as it appears to be from the images, it may not be possible or easy to develop an algorithm to detect cirrus, or to distinguish other thin clouds from haze. We also noted that the IR systems appeared to have more noise. At least the IR imagers available at the time were also fairly low resolution, except possibly for imagers that are far more costly than the visible imagers. In Section 9.4, we further explore these impressions from a theoretical point of view. First, however, we would like to comment briefly on the Mid Wave IR (MWIR).

9.3. Comments Regarding Mid Wave IR Systems

We are not aware of any groups attempting to provide routine whole sky cloud monitoring using a Mid-wave IR (MWIR) system operating in the 3 – 5 μm range. However one of the IR camera manufacturers, Electrophysics, sent us sample narrow-angle images taken in the 3 – 5 μm region and the 8 – 12 μm region, as shown in Figures 26 and 27. Both images were sent courtesy of C. Alicandro at Electrophysics.



Fig. 26. Sample cloud image taken with a cooled camera operating in the 3 - 5 μm region.



Fig. 27. Sample cloud image taken with an uncooled camera operating in the 8 – 12 μm region.

From an evaluation of the energy levels, scattering and absorption mechanisms, we feel that development of algorithms for the MWIR might be significantly more difficult than development of algorithms for either the visible or the LWIR. Whereas the visible cloud detection is driven primarily by scattering, and the LWIR cloud detection is driven primarily by absorption and emission, the MWIR is impacted significantly by both mechanisms (Zissis 1993, see Fig. 3.19). This is partly because the solar radiance is fairly high in the MWIR. For example, Holst 2000 indicates that the solar ground irradiance is about 24 W/m^2 , while the self-emission of a 290k blackbody is 4.1 W/m^2 in the 3 – 5 μm range. This may also imply that a solar occulter would be necessary in the MWIR, whereas it is not in the LWIR. We decided not to evaluate the MWIR further at this time for these reasons.

9.4. Theoretical Study of LWIR Characteristics

For the theoretical study, our goal was to evaluate how much the background sky signature on a LWIR whole sky image might be expected to vary, and how the cloud signature should compare with the background sky. More specifically, we wanted to know whether there was sufficient difference in the signals to detect the clouds, and if so, whether a cloud algorithm beyond a simple threshold would be required. In order to have a better understanding, we wanted to derive this from the basic physics, although we would like to make a more extensive evaluation in the future using standard atmospheric models.

9.4.1. Discussion of the Approach

Although the source of the cloud signal is the thermal emission of the clouds, the signal is not just that due to the temperature of the clouds. The radiance that reaches the sensor is also impacted by the transmittance of the path of sight between the ground and the cloud, and the path radiance, or radiance scattered into the path of sight from the surround. The apparent radiance of any target t at range r may be given as

$$L_r(\theta, \phi) = L_0(\theta, \phi) * T_r(\theta) + L_p(\theta, \phi) \quad (1)$$

where

$L_r(\theta, \phi)$ is the target radiance from range r at zenith angle θ and azimuth angle ϕ ,
 $L_0(\theta, \phi)$ is the target radiance from range 0 at zenith angle θ and azimuth angle ϕ ,
 $T_r(\theta)$ is the beam transmittance over the path from r to 0 at zenith angle θ , and
 $L_p(\theta, \phi)$ is the path radiance between the observer and the target at zenith angle θ and azimuth angle ϕ .

The transmittance losses are very significant in the LWIR. For example, see Holst 2000 Figure 5-4, which illustrates that the transmittance at 10 μm is on the order of .5 over a 2 km path length, and less than .1 over a 10 km path length. Also, the path radiance may be very significant in the LWIR. For example, see Holst 2000 Figure 5-8, which shows an example of an image taken near the St. Louis Gateway Arch of path radiance due to aerosol layers.

The LWIR sensors often are calibrated in Blackbody temperature in degrees (as in Fig. 27). After exploring a variety of theoretical approaches to our problem, we took the following approach to calculating the cloud signature:

- a) Determine typical cloud altitudes of interest, and the associated temperatures
- b) Calculate the relative radiance for these temperatures
- c) Correct for beam transmittance
- d) Correct for path radiance

- e) Convert back to effective temperature
- f) Compare with the effective temperature of the backgrounds.

This will be discussed in more detail in the following sections.

9.4.2. Cloud Signatures, Part 1

Zissis 1993 (page 226) lists typical cloud altitudes in temperate regions as shown in Table 1, Column 2. For our sample calculations, we used the altitudes shown in Column 3. The standard atmosphere temperatures (McCartney 1976 Table 2.6) were rounded to the nearest 5°, and are shown in Column 4. Temperature extremes for 60° N Latitude in winter and 30° N Latitude in summer were extracted from McCartney 1976 Appendix F, and are shown in Columns 5 and 6.

Table 1
Cloud Altitudes used in Calculations

Cloud Layer	Zissis Altitude Range	Altitude used For calculations	Temperatures Evaluated, ° K		
			Standard Atmosphere Approximate Temp	Cold Extreme 60° North Winter	Warm Extreme 30° North Summer
Low	0 – 2 km	1 km	270	257	301
Mid	2 – 7 km	5 km	260	241	272
High	5 – 13 km	10 km	225	217	238

To calculate the relative radiance for these clouds, we used the blackbody equation for radiative exitance shown in Eq. 2, as stated by Holst 2000 and Zissis 1993 Chapter 1.

$$M(\lambda, T) = \frac{c_1}{\lambda^5} \left[\frac{1}{e^{c_2/\lambda T} - 1} \right] \frac{W}{m^2 - \mu m} \quad (2)$$

where:

M=Blackbody radiant exitance in W m⁻² μm⁻¹
c₁ = 3.7411 10⁸ W μm⁴ / m² (radiation constant)
c₂ = 1.4388 10⁴ μm K (radiation constant)
λ = wavelength in micrometers
T = temperature in degrees Kelvin

(Be careful not to confuse T, which is used for Temperature in Eq. 2, with T_r which is used for transmittance in Eq. 1.) For our calculations, we used a wavelength of 10 μm, and used the exitance for all calculations, for consistency. Although this is not equal to radiance, it should be proportional to radiance, and can be used if we are careful in the handling not to mix units.

We also wanted to take into account the emissivity of the clouds, which describes the efficiency with which objects radiate in comparison with a blackbody. From equations given in Jacobs 1996, we estimate that the emissivity should be very close to 1 for the opaque clouds. (Jacobs also reports the emissivity of the sky with values ranging from about .2 to about .77, if we interpret him correctly.) We decided to make our calculations using values of 1 for the low and the middle clouds. For high clouds, we used 1 for opaque clouds, and .5 for thin clouds. By using a value of 1, we are reporting the best possible behavior, in the sense that this would provide the best contrast for the IR imager that is trying to detect the clouds. That is, we are being somewhat conservative in making the IR system look as good as possible.

The next step is to determine the transmittance for use in Eq. 1. To do this, we first extracted typical transmittances at $10\text{ }\mu\text{m}$ over horizontal paths of 1 km, 2 km, and 5 km from Holst 2000. We verified that the values yielded a consistent scattering coefficient at $10\text{ }\mu\text{m}$ near ground level of about $.35\text{ km}^{-1}$, and also verified in other references that this value is reasonable. For the 1 km horizontal path, the resulting transmittance is about .70.

The relationship between a horizontal transmittance and a vertical transmittance is complex and variable, as it depends on the structure of the haze layers. To estimate reasonable bounds on the vertical transmittance in relation to the horizontal transmittance, we used measurements of vertical profiles of scattering coefficient taken by our group from aircraft (Duntley et al. 1978). A sample scattering coefficient profile is shown in Figure 28.

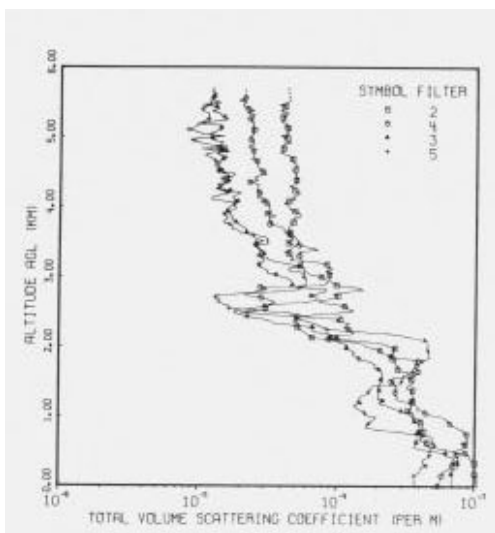


Fig. 28. Vertical profile of scattering coefficients from Duntley et al. 1978.

The Duntley report includes the ground-based scattering coefficients, as well as the beam transmittance computed from ground to altitude using the measured scattering coefficient profiles. From this flight data, we found that a vertical path from the ground to 1 km sometimes has a higher, and sometimes lower, transmittance than the horizontal path of 1

km. For a vertical path from the ground to 5 km and 10 km, we found that the transmittance was about an average factor of .65 lower (for 5 km) and .52 lower (for 10 km). Thus we estimated a reasonable vertical transmittance to 1, 5, and 10 km at .70, .46, and .36 as shown in Table 2. This is clearly an area where it would be useful to evaluate the results with model scattering coefficient lapse rates, but we felt that for now this approach would provide a reasonable assessment.

Table 2
Estimated Vertical Beam Transmittance
Using a Horizontal Transmittance over 1 km of .70

Cloud Altitude	Vertical Tr Divided by Horizontal 1 km Tr	Estimated Vertical Transmittance
1 km	1	.70
5 km	.65	.46
10 km	.52	.36

To evaluate the cloud signatures at non-vertical look angles, we used the equation

$$T_r(\theta) = T_r(0)^{|\sec \theta|} \quad (3)$$

The next step is correcting for path radiance. However, we first would like to discuss the clear sky background signatures, because we based the path radiance calculation on these signatures.

9.4.3. Background Signatures

In evaluating quite a range of references, we considered either using measured background signatures directly, or computing the signatures from other values such as the effective emissivity of the atmosphere. Eventually, we decided to use a very simple approach. Holst 2000 reports that a good rule of thumb for typical atmospheres is that the effective temperature of the sky in the 8 – 12 μm region is near 260° K overhead, and near 293° K at the horizon, with a net variation of 33° K from the horizon to the zenith. Furthermore, these temperatures vary with the ambient temperature.

We decided to use this information, and supplement it with information on how much the ambient temperature might be expected to vary. Clearly, it would be good to do a more extensive modeling study using Modtran in the future, but again we felt that this physical approach would yield a better understanding of the variations in IR imagery and their causes. We evaluated this rule of thumb in comparison with the sky measurements of Jacobs 1996, and found them to be reasonably consistent, although Jacobs shows a larger range of 49° K from horizon to zenith.

We looked at quite a few sources to evaluate how much these temperatures might be expected to vary. First we looked at seasonal variations. From McCartney 1976, the ground temperature monthly means from winter at 60° N to summer at 30° N vary from 257° K to 301° K, for a net range of $\pm 22^\circ$ K. Moran and Morgan 1991 list typical CONUS (Continental US) ground temperatures as 265° K to 292° K in winter, and 292° K to 312° K in summer, yielding a net variation in CONUS of $\pm 24^\circ$ K.

In addition, there are diurnal variations. Moran and Morgan 1991 list typical diurnal variations from the normal daily maximum to the normal daily minimum as about $\pm 8^\circ$ in the winter, and $\pm 7^\circ$ in the winter.

In addition, there is significant variation as a result of changes in aerosol and air mass. For example, in Zissis 1993, Figures 3.22 and 3.23 show the spectral irradiance of a clear nighttime sky for several angles of elevation above the horizon for stations in Colorado and in Florida. Extracting the approximate spectral radiance in $\mu\text{W cm}^{-2} \text{sr}^{-1} \mu\text{m}^{-1}$ near 10 μm from the plots, we find the following. The spectral radiance at the zenith is about 60 for Colorado and about 260 for Florida, and the spectral radiance near the horizon is about 807 for Colorado and about 920 for Florida. In this example, the aerosol and air mass made a very significant difference, especially at the zenith.

Some of the implications of these background signatures are as follows. Within a single image, the effective background temperatures will be significantly higher at the horizon than the zenith, with deltas of about 33 to 49° K, and potentially different variations depending on air mass and aerosol considerations. From one image to another, we can expect diurnal variations of roughly ± 22 to 24° K, and diurnal variations of roughly ± 7 to 8° K. Overall, taking the zenith to horizon range of 260 to 293° K from Holst 2000, and adding these seasonal and diurnal variations, that means the sensor can expect to see effective background temperatures ranging from about 228 to 325° K, if the extremes and the differences in aerosol are not considered. We got detailed specifications on 3 cameras that would be reasonable to consider for this application, and their minimum temperature readings, at the time of this study, were 257, 257, and 237° K. We will use an estimated minimum of 247° K for this study. This implies that for some environments, the background sky signature may be offscale dark, and thus very thin clouds may also be offscale dark.

For our calculations, we wished to calculate the cloud and the background signatures for low, middle, and high clouds, as defined in Table 1. We included computations for the standard atmosphere, 60° N winter, and 30° N summer. At the time of this study, we were told that we would like to sense to 0 to 5° above the horizon (85 - 90° zenith angle), and must sense down to at least 20° above the horizon (70° zenith angle). Knowing that requirements are sometimes compromised, we decided to calculate the IR signatures for zenith angles of 0°, 60°, and 85° zenith angles. We based the ground temperature variations on McCartney 1976, and the zenith angle effective temperature variations on Holst 2000. The result was the effective background temperatures shown in Table 3.

Table 3
Effective Radiating Temperatures used for Sky Backgrounds

Zenith Angle	Standard Atm	Winter 60 N	Summer 30 N
0°	260°	224°	268°
60°	283°	247°	291°
85°	291°	255°	299°

9.4.4. Cloud Signatures, Part 2

The remaining step in the cloud signature calculation was applying the correction for the path radiance. The effective background temperatures discussed in Section 9.4.3 are essentially the temperatures that correspond to the path radiance from earth to space. The path radiance from ground to altitude should be less than the path radiance from ground to space, although they should be quite close for high altitudes. The largest contribution to the path radiance will be from the lower warmer layers, so even for the lower cloud altitudes, the path radiance may not be that much less than the earth to space path radiances.

We decided to use the ground-to-space path radiances derived from the background temperatures in calculating the cloud signatures, for two reasons. First, the ground-to-space path radiance bounds the problem, and we do not expect large differences between the ground-to-space and most ground-to-altitude path radiances, as discussed above. Second, if we have an error in our background radiances, it will affect both the cloud and background radiances equally, and thus have minimal effect on the conclusions. By doing this, we are once again taking a very conservative approach, i.e. calculating performance of the IR sensors that is better than the real performance, because by using a path radiance higher than the true path radiance, the calculations will yield higher contrast with the background than would actually be obtained.

To illustrate how this information is put together, we provide a sample calculation. For an opaque cloud at 10 km at the zenith in the standard atmosphere, we use a cloud temperature of 225 K (Table 1). Using Eq. 2 yields a relative radiance of 6.26. The emittance of the cloud is estimated to be near 1. The transmittance for the zenith direction and a cloud altitude of 10 km is estimated to be .36 (Table 2). The product of the relative radiance, emittance, and transmittance yields a transmitted relative radiance of 2.25. The background effective temperature, from Table 3, is estimated to be 260 K. Using Eq. 2 to convert this to a relative radiance yields a relative path radiance of 14.8. Using Eq. 1 to combine the transmitted relative radiance and the relative path radiance yields a net effective radiance for the cloud of 17.1. Using the inverse of Eq. 2 to derive the effective temperature corresponding to this relative radiance yields an effective temperature for the cloud, as detected from the ground, of 266.8 K.

9.4.5. Resulting Cloud and Background Effective Temperatures

The results of the calculations are shown in Tables 4 – 6. In each of these tables, the cloud altitude and zenith angle are shown in Columns 1 and 2. Columns 3, 5, and 7 show the effective temperatures for the clouds, as sensed from the ground, and columns 4, 6, and 8 show the temperature difference between the cloud and the background. In the bottom row, we show the background effective temperature, as sensed from the ground, and extracted from Table 3. The colors used in the table will be explained below.

Table 4
Computed Cloud and Background Results for the Zenith
(Colors explained in Text)

		Standard Atm		Winter 60N		Summer 30N	
Alt (km)	Zen	Eff Temp	ΔT	Eff Temp	ΔT	Eff Temp	ΔT
1	0	298.2	38.2	263.0	39.0	315.8	47.8
5		279.0	29.0	244.7	20.7	289.7	21.7
10		266.8	6.8	233.3	9.3	276.6	8.6
10 Thin		263.5	3.5	228.9	4.9	272.4	4.4
Aerosol		260.0		224.0		268.0	

There are four colors used in these tables. The light blue cells are cases where the cloud signal is lower than the anticipated minimum sensitivity range of 247K for the IR sensor. That is, in these cases, we expect the signal to be offscale dark, and it should not be possible to sense the clouds or background. These cases occur in the Winter 60° N case for the zenith. At 60° zenith angle, the clouds have come onscale, but the background is still offscale dark, so that algorithm development would be difficult.

In Table 4, there are 3 cells that are colored yellow. Yellow indicates those cases for which the difference between the cloud and the background is greater than the variation in background from the zenith to 85° zenith angle. For example, in the standard atmosphere, the difference in the background between 0 and 85° zenith angle was estimated to be 31° K (Table 3). The low altitude clouds are about 38° K warmer than the background. Thus, they should be detectable with a simple threshold cloud algorithm. However, the clouds at other altitudes, as well as other zenith angles, have less temperature difference from their background. For all the cases **not** marked with yellow, we do not expect a simple threshold to work well, because it will either miss most of the clouds, or call the horizon a cloud.

Table 5
Computed Cloud and Background Results for 60° Zenith Angle
(Colors explained in Text)

		Standard Atm		Winter 60N		Summer 30N	
Alt (km)	Zen	Eff Temp	ΔT	Eff Temp	ΔT	Eff Temp	ΔT
1	60	305.7	22.7	269.1	22.0	320.3	29.3
5		290.1	7.1	254.3	7.3	299.3	8.3
10		284.9	1.9	249.4	2.4	293.5	2.5
10 Thin		284.0	1.0	248.2	1.2	292.2	1.2
Aerosol		283.0		247.0		291.0	

Table 6
Computed Cloud and Background Results for 85° Zenith Angle
(Colors explained in Text)

		Standard Atm		Winter 60N		Summer 30N	
Alt (km)	Zen	Eff Temp	ΔT	Eff Temp	ΔT	Eff Temp	ΔT
1	85	291.8	0.8	255.8	0.78	300.1	1.06
5		291.0	.004	255.0	.005	299.0	.005
10		291.0	.00007	255.0	.0001	299.0	.001
10 Thin		291.0	.00002	255.0	.00007	299.0	.00008
Aerosol		291.0		255.0		299.0	

In Table 4, there are 4 cells marked with a light pink. These are cases where the difference between the cloud and the background is less than $\frac{1}{4}$ of the 31° K range in the background. These are cases where the algorithm would have to be reasonably sophisticated. The algorithm would need to detect a delta that is somewhat small in comparison with the variation within an image. The difference between the cloud and the

background is even smaller in comparison with the background variation from image to image. The need to take into account seasonal, diurnal, and other variations in the background signal would make the algorithm more complicated.

In Table 5, and 60° zenith angle, all of the middle and high clouds except for one summer 30° latitude case are colored light pink, indicating that we would expect a reasonably sophisticated algorithm to be needed to automatically recognize the clouds.

In Table 6, there is a dark pink category. This represents the cases where the temperature differences between the cloud and background are less than the NEDT (Noise Equivalent Delta Temperature) for the sensors we evaluated. That is, the clouds are buried in the system noise, and would not be detected, according to these calculations.

Thus these calculations imply that for the conditions we studied, the IR sensor would not sense middle or high clouds near the horizon. The sensor would require a reasonably sophisticated algorithm to identify the presence of middle and high clouds at other angles. At the zenith, identifying the presence of low clouds would be simple, and even without a sophisticated algorithm. Middle and high clouds at the zenith would require a sophisticated algorithm, and may be offscale dark at the zenith in winter in cold environments.

Clearly, this is not a definitive study, and ideally we would like to expand the study both with measurements and with modeling studies. However, we feel that these results give us some understanding of what to expect from IR systems, and why. We were pleased that our sponsors indicated that these results fit very well with experimental results they have seen but that have not been published.

9.5. Summary of the Wavelength Analysis

As discussed in Section 9.1, we do not believe that sensors at 1.6 μm will do a better job for our application, because these cameras tend to provide a poorer image, and we do not believe their sensitivity will be adequate for night-time applications. We did not evaluate MWIR sensors in detail, because they appear not to provide any significant benefits, and the algorithms would be more complex.

There are some LWIR systems in development, and at this point, their imagery does not appear to be as good as that obtained in the visible. A theoretical analysis of the cloud and background signals indicates that although low clouds at the zenith are easy to detect, sophisticated algorithms will probably be required to detect low clouds at angles away from the zenith. Also, a reasonably sophisticated algorithm will probably be required to detect middle and high clouds at most angles. Close to the horizon, middle and high clouds are expected to be buried in the noise. In cold environments, the middle and high clouds at the zenith may be offscale dark.

In order to successfully identify the presence of clouds, two things are necessary. First, the raw imagery must have sufficient difference between the cloud and background

signals. Second, algorithms must be able to sort out these differences and identify the presence of the clouds. Our initial analysis leads us to believe that for an IR system, the first constraint may not occur for many needed angles and cloud heights, and reasonably sophisticated algorithms will be required for most angles and cloud heights. By contrast, as illustrated in earlier sections, the visible sensors provide very high quality imagery, and clouds are well detected down to the horizon, and at all cloud altitudes.

If cost constraints limit the application to a single sensor, we feel that the visible sensors will be very much superior, because they have already demonstrated that they can detect high and low clouds night and day, overhead and near the horizon, some of which may be offscale or in the noise for IR sensors at the present time. Furthermore, the algorithms are much more developed than the IR system algorithms we are aware of at the present time, although the algorithms are continuing to be advanced even in the visible.

Also, because the transmission losses at 1.6 μm are primarily driven by scattering mechanisms, like the visible, whereas the thermal IR cloud detection is based on thermal emission, we feel we have a better chance of detecting the clouds of importance to the SWIR. We make these statements with the caveat that it may at some point become a priority to further evaluate these beliefs, using measurements and modeling studies. In particular, we note that it may turn out that a hybrid system, using both a visible and an IR sensor, though much more costly, could provide enough advantage to be worth evaluating.

10. Summary

During this contract period, significant progress was made in providing day and night algorithms, in providing WSI hardware and maintenance, and in evaluation of the best wavelength regimes to use for the application. We believe that we have completed all contract requirements.

11. Acknowledgements

We would like to express our appreciation to the personnel of Starfire Optical Range and their contractors from Boeing. Dr. Earl Spillar, the head of this program, Ann Slavin, our acting contract monitor, and Dr. Robert Fugate, the director of SOR at the time of this contract, were all helpful, and have been a pleasure to work with. We feel this work is valuable, and very much appreciate having had the chance to advance the state of the art, as well as meet our sponsor's specific needs. We also would like to express our appreciation to ONR, which provided the funding vehicle for this work.

12. References

In-house Technical Memoranda, in order by memo number; available to sponsor on request

Karr, M., "Unit 12 Software Updates", Atmospheric Optics Group Technical Memorandum AV01-029t, 29 January 2001

Karr, M., "Update to ProcWSI for Unit 13/14", Atmospheric Optics Group Technical Memorandum AV01-030t, 29 January 2001

Shields, J., "SOR Trip Report, Jan '01", Atmospheric Optics Group Technical Memorandum AV01-031t, 28 February 2001

Shields, J., "Procedure for Processing SOR Cloud Library Data", Atmospheric Optics Group Technical Memorandum AV01-032t, 28 February 2001

Karr, M., "SOR RunWSI Updates", Atmospheric Optics Group Technical Memorandum AV01-033t, 28 February 2001

Karr, M., "SOR ProcWSI Updates", Atmospheric Optics Group Technical Memorandum AV01-034t, 28 February 2001

Shields, J., "SOR Clear Sky Background Library File Generation for Unit 12", Atmospheric Optics Group Technical Memorandum AV01-035t, 6 April 2001

Burden, A. R., "Basic Geometric Calibration of WSI Unit 12", Atmospheric Optics Group Technical Memorandum AV01-041t, 10 June 2001

Burden, A. R., "Unit 12 Rolloff Calibration", Atmospheric Optics Group Technical Memorandum AV01-042t, 18 June 2001

Burden, A. R., "Unit 12 Flat Field Calibration", Atmospheric Optics Group Technical Memorandum AV01-043t, 23 June 2001

Burden, A. R., "Unit 12 Linearity and Exposure Calibration Results", Atmospheric Optics Group Technical Memorandum AV01-044t, 23 June 2001

Burden, A. R., "Unit 12 Effective Lamp Irradiance Computation", Atmospheric Optics Group Technical Memorandum AV01-045t, 20 June 2001

Burden, A. R., "Unit 12 Aperture Calibrations", Atmospheric Optics Group Technical Memorandum AV01-046t, 22 June 2001

Burden, A. R., "Absolute Calibration Results for Unit 12", Atmospheric Optics Group Technical Memorandum AV01-047t, 20 June 2001

Burden, A. R., “Unit 12 Calibration Summary”, Atmospheric Optics Group Technical Memorandum AV01-048t, 27 June 2001

Burden, A. R., “Basic Geometric Calibration of WSI Unit 13”, Atmospheric Optics Group Technical Memorandum AV01-049t, 10 June 2001

Burden, A. R., “Unit 13 Rolloff Calibration”, Atmospheric Optics Group Technical Memorandum AV01-050t, 28 June 2001

Burden, A. R., “Unit 13 Flat Field Calibration”, Atmospheric Optics Group Technical Memorandum AV01-051t, 27 June 2001

Burden, A. R., “Unit 13 Linearity and Exposure Calibration Results”, Atmospheric Optics Group Technical Memorandum AV01-052t, 26 June 2001

Burden, A. R., “Unit 13 Effective Lamp Irradiance Computation”, Atmospheric Optics Group Technical Memorandum AV01-053t, 22 June 2001

Burden, A. R., “Unit 13 Aperture Calibrations”, Atmospheric Optics Group Technical Memorandum AV01-054t, 26 June 2001

Burden, A. R., “Unit 13 Acrylic Dome Calibration”, Atmospheric Optics Group Technical Memorandum AV01-055t, 26 June 2001

Burden, A. R., “Absolute Calibration Results for Unit 13”, Atmospheric Optics Group Technical Memorandum AV01-056t, 26 June 2001

Burden, A. R., “Unit 13 Calibration Summary”, Atmospheric Optics Group Technical Memorandum AV01-057t, 29 June 2001

Burden, A. R., “Basic Geometric Calibration of WSI Unit 14”, Atmospheric Optics Group Technical Memorandum AV01-058t, 10 June 2001

Burden, A. R., “Unit 14 Rolloff Calibration”, Atmospheric Optics Group Technical Memorandum AV01-059t, 29 June 2001

Burden, A. R., “Unit 14 Flat Field Calibration”, Atmospheric Optics Group Technical Memorandum AV01-060t, 27 June 2001

Burden, A. R., “Unit 14 Linearity and Exposure Calibration Results”, Atmospheric Optics Group Technical Memorandum AV01-061t, 27 June 2001

Burden, A. R., “Unit 14 Effective Lamp Irradiance Computation”, Atmospheric Optics Group Technical Memorandum AV01-062t, 27 June 2001

Burden, A. R., “Unit 14 Aperture Calibrations”, Atmospheric Optics Group Technical Memorandum AV01-063t, 27 June 2001

Burden, A. R., “Unit 14 Acrylic Dome Calibration”, Atmospheric Optics Group Technical Memorandum AV01-064t, 27 June 2001

Burden, A. R., “Absolute Calibration Results for Unit 14”, Atmospheric Optics Group Technical Memorandum AV01-065t, 27 June 2001

Burden, A. R., “Unit 14 Calibration Summary”, Atmospheric Optics Group Technical Memorandum AV01-066t, 29 June 2001

Burden, A. R., “CalWSI_FlatField – IDL Software for Flat Field and Rolloff Calibrations”, Atmospheric Optics Group Technical Memorandum AV01-067t, 29 June 2001

Baker, J., “Unit 13 Trolley Failure”, Atmospheric Optics Group Technical Memorandum AV01-068t, 27 June 2001

Shields, J., “Research Approach for High Resolution Night Cloud Algorithms”, Atmospheric Optics Group Technical Memorandum AV01-069t, 3 July 2001

Shields, J., “Return of SOR Unit 14 from Northern California, 3 July 01”, Atmospheric Optics Group Technical Memorandum AV01-070t, 10 July 2001

Shields, J., “Unit 13 Parts List”, Atmospheric Optics Group Technical Memorandum AV01-080t, 6 September 2001

Karr, M., “SOR Unit 13 and 14 run time history”, Atmospheric Optics Group Technical Memorandum AV01-092t, 28 September 2001

Shields, J., “Camera Shutter Delays under Windows and SOR Software”, Atmospheric Optics Group Technical Memorandum AV01-094t, 2 October 2001

Shields, J. and A. Burden, “Derivation of Star Irradiance for the Beam Transmittance Project”, Atmospheric Optics Group Technical Memorandum AV01-097t, 9 October 2001

Burden, A., “Improvements Made to Starlight-Based WSI Cloud Algorithm”, Atmospheric Optics Group Technical Memorandum AV03-030t, 19 May 2003

Burden, A., “ImgCal: New Software for the Radiometric Calibration of D/N WSI Images”, Atmospheric Optics Group Technical Memorandum AV03-037t, 9 September 2003

Karr, M., “Control Computer operations overview for WSI units 13 and 14, Version 4.2”, Atmospheric Optics Group Technical Memorandum AV03-047t, 06 November 2003

Karr, M., “Display/Processing Computer operations overview for WSI Units 13 and 14, Version 2.1.”, Atmospheric Optics Group Technical Memorandum AV03-048t, 06 November 2003

Baker, J., “Filter Changing Alignment Procedure for SOR Unit 12”, Atmospheric Optics Group Technical Memorandum AV03-049t, 07 November 2003

Baker, J., “SOR WSI Unit 12 Field Diagnostics and Repair Trip – October 2003”, Atmospheric Optics Group Technical Memorandum AV03-052t, 24 November 2003

Baker, J., and J. Shields, “SOR-TASC Virginia Unit 14 Install Trip – November 2003”, Atmospheric Optics Group Technical Memorandum AV03-054t, 04 December 2003

Baker, J., “Acrylic Dome Installation Procedure”, Atmospheric Optics Group Technical Memorandum AV03-055t, 08 December 2003

Baker, J., “Unit 13 and 14 Trolley Calibration and Alignment Procedure (Revised)”, Atmospheric Optics Group Technical Memorandum AV03-056t, 12 December 2003

Baker, J., “Unit 13 & 14 Trolley Cart Removal and Fixed Shade Installation Procedure”, Atmospheric Optics Group Technical Memorandum AV04-001t, 08 January 2004

Shields, J., “Unit 14 Radiometric Calibrations”, Atmospheric Optics Group Technical Memorandum AV04-002t, 19 January 2004

Burden, A., “Earth-To-Space Beam Transmittance from Nighttime WSI Imagery: Preliminary Results”, Atmospheric Optics Group Technical Memorandum AV04-004t, 20 January 2004

Shields, J., “Unit 14 Parts list and Overview”, Atmospheric Optics Group Technical Memorandum AV04-007t, 25 March 2003

Baker, J., “Upgrading the WSI flow package from Series 100 to Series 800”, Atmospheric Optics Group Technical Memorandum AV04-009t, 08 April 2004

Baker, J., “Unit 12 Arc Calibration and Alignment Procedure Revisited”, Atmospheric Optics Group Technical Memorandum AV04-010t, 08 April 2004

Baker, J., “Unit 12 Trolley Calibration and Alignment Procedure Revisited”, Atmospheric Optics Group Technical Memorandum AV04-011t, 08 April 2004

Shields, J., “Summary of the NIR Day Cloud Algorithm for the German Day WSI”, Atmospheric Optics Group Technical Memorandum AV04-014t, 9 Apr 2004

Baker, J., "Unit 13 & 14 Environmental Housing Temp Sensor Replacement", Atmospheric Optics Group Technical Memorandum AV04-019t, 07 May 2004

Shields, J., "Shutter Tests with Windows-based D/N WSI Systems using Units 13 and 2", Atmospheric Optics Group Technical Memorandum AV04-024t, 21 May 2004

Burden, A., "Unit 13 Effective Lamp Radiances for Field Calibration", Atmospheric Optics Group Technical Memorandum AV04-025t, 28 May 2004

Baker, J., "WSI System Checklist for Unit 13&14", Atmospheric Optics Group Technical Memorandum AV04-026t, 01 June 2004

Burden, A., "Unit 13 Field Calibration Results", Atmospheric Optics Group Technical Memorandum AV04-027t, 02 June 2004

Baker, J., "Filter Changer Alignment procedure for SOR Unit 13&14", Atmospheric Optics Group Technical Memorandum AV04-029t, 09 July 2004

Karr, M., "Revised Field calibration program, Fieldcal for Windows Version 1.0", Atmospheric Optics Group Technical Memorandum AV04-030t, 16 July 2004

Baker, J., "Trolley Drive Gear and Chain Adjustment Procedures – Unit 13&14", Atmospheric Optics Group Technical Memorandum AV04-031t, 20 July 2004

Baker, J., "Unit 14 SOR/TASC Virginia Trip – Trolley Drive Analysis and Repair 4/12/04", Atmospheric Optics Group Technical Memorandum AV04-032t, 20 July 2004

Baker, J., "Unit 13 Updated parts List and Overview", Atmospheric Optics Group Technical Memorandum AV04-033t, 20 July 2004

Baker, J., "Unit 14 Updated Parts List and Overview", Atmospheric Optics Group Technical Memorandum AV04-034t, 20 July 2004

Baker, J., "Unit 14 SOR/TASC Virginia Trip – Camera Install and FC Repair 6/7/04", Atmospheric Optics Group Technical Memorandum AV04-035t, 20 July 2004

Shields, J., "Processing of SGP Feb 02 Data for Cloud Decision", Atmospheric Optics Group Technical Memorandum AV04-038t, 31 August 2004

Shields, J., "Processing of SGP Mar 02 Data for Cloud Decision", Atmospheric Optics Group Technical Memorandum AV04-039t, 31 August 2004

Karr, M., "Image Utility Programs", Atmospheric Optics Group Technical Memorandum AV04-043t, 22 September 2004

Baker, J., “Procedure for Changing WSI Shutter in Units 13&14”, Atmospheric Optics Group Technical Memorandum AV04-044t, 28 September 2004

Burden, A., “Unit 14v1 and 13v2 Effective Lamp Radiances for Field Calibration”, Atmospheric Optics Group Technical Memorandum AV04-045t, 12 August 2004

Burden, A., “Unit 14v1 and 13v2 Field Calibration Results”, Atmospheric Optics Group Technical Memorandum AV04-046t, 12 August 2004

Shields, J., “Abnormal Red/blue ratios in Aug 02 SGP D/N WS Data Set”, Atmospheric Optics Group Technical Memorandum AV04-047t, 14 October 2004

Shields, J., “Processing of SGP August 02 Data for Cloud Decision”, Atmospheric Optics Group Technical Memorandum AV04-049t, 23 October 2004

Shields, J., “Reprocessing of SGP Feb and Mar 02 Data for Cloud Decision”, Atmospheric Optics Group Technical Memorandum AV04-050t, 03 November 2004

Shields, J., “Initial Virginia night data analysis”, Atmospheric Optics Group Technical Memorandum AV04-054t, 31 December 2004

Published References and Technical Notes in order by date

McCartney, Earl J., (1976), “Optics of the Atmosphere – Scattering by Molecules and Particles”, Wiley Series in Pure and Applied Optics, Stanley S. Ballard, Advisory Editor, John Wiley and Sons, New Your, London, Sydney, Toronto

Duntley, Seibert Q., R. W. Johnson, and J. I. Gordon (1978), “Airborne Measurements of Atmospheric Volume Scattering Coefficients in Northern Europe, Summer, 1977”, Visibility Laboratory, Scripps Institution of Oceanography, University of California San Diego, SIO 78-28, AFGL-TR-78-0168

Hobbs, Peter V., and Adarsh Deepak, (1981), “Clouds, Their Formation, Optical Properties, and Effects”, Academic Press, A Subsidiary of Harcourt Brace Jovanovich, Publishers, New York, London, Toronto, Sydney, San Francisco. We referenced articles in this book by James Jiusto and by Stephen K. Cox.

Johnson, R. W., W. S. Hering and J. E. Shields (1989), “Automated Visibility and Cloud Cover Measurements with a Solid-State Imaging System”, Marine Physical Laboratory, Scripps Institution of Oceanography, University of California San Diego, SIO 89-7, GL-TR-89-0061, NTIS No. ADA216906

Johnson, R. W., J. E. Shields, and T. L. Koehler (1991), “Analysis and Interpretation of Simultaneous Multi-Station Whole Sky Imagery”, Marine Physical Laboratory, Scripps Institution of Oceanography, University of California San Diego, SIO 91-3, PL-TR-91-2214

Moran, Joseph M., and Michael D. Morgan, (1991), “Meteorology – The Atmosphere and The Science of Weather”, Third Edition, Macmillan Publishing Company, New York, and Collier Macmillan Canada, Toronto

Shields, J. E., R. W. Johnson, and T. L. Koehler, (1993), “Automated Whole Sky Imaging Systems for Cloud Field Assessment”, Fourth Symposium on Global Change Studies, 17 – 22 January 1993, American Meteorological Society, Boston, MA

Zissis, George J., Editor (1993), “Volume 1: Sources of Radiation” of “The Infrared and Electro-Optical Systems Handbook, Joseph S. Accetta and David L. Shumaker Executive Editors, Copublished by Infrared Information Analysis Center, Environmental Research Institute of Michigan, Ann Arbor, Michigan, and by SOIE Optical Engineering Press, Bellingham, Washington, USA. We referenced Chapter 1 by William Wolfe, and Chapter 3 by David Kryskowski and Gwynn Suits.

Shields, J. E., R. W. Johnson, and M. E. Karr, (1994), “Upgrading the Day/Night Whole Sky Imager from Manual/Interactive to Full Automatic Control, Marine Physical Laboratory, Scripps Institution of Oceanography, University of California San Diego, Report MPL-U-140/94

Jacobs, Pieter A., (1996), “Thermal Infrared Characterization of Ground Targets and Backgrounds”, Tutorial Texts in Optical Engineering volume TT26, Donald O’Shea Series Editor, SPIE Optical Engineering Press, A Publication of SPIE – The International Society for Optical Engineering, Bellingham, Washington

Shields, J. E., R. W. Johnson, M. E. Karr, R. A. Weymouth, and D. S. Sauer, (1997a), “Delivery and Development of a Day/Night Whole Sky Imager with Enhanced Angular Alignment for Full 24 Hour Cloud Distribution Assessment”, Marine Physical Laboratory, Scripps Institution of Oceanography, University of California San Diego, Report MPL-U-8/97

Shields, J. E., M. E. Karr, and R. W. Johnson, (1997b), “Service Support for the Phillips Laboratory Whole Sky Imager”, Marine Physical Laboratory, Scripps Institution of Oceanography, University of California San Diego, Report MPL-U-10/97

Shields, J. E., R. W. Johnson, M. E. Karr, and J. L. Wertz, (1998), “Automated Day/Night Whole Sky Imagers for Field Assessment of Cloud Cover Distributions and Radiance Distributions”, Tenth Symposium on Meteorological Observations and Instrumentation, 11 – 16 January 1998, American Meteorological Society, Boston, MA

Feister, U., Shields, J., Karr, M., Johnson, R., Dehne, K. and Woldt, M, (2000), “Ground-Based Cloud Images and Sky Radiances in the Visible and Near Infrared Region from Whole Sky Imager Measurements”, Proceedings of Climate Monitoring – Satellite Application Facility Training Workshop sponsored by DWD, EUMETSAT and WMO, Dresden 2000.

Holst, Gerald C., (2000), “Common Sense Approach to Thermal Imaging” Copublished by JCD Publishing, Winter Park, Florida, and SPIE Optical Engineering Press, A Publication of SPIE – The International Society for Optical Engineering, Bellingham, Washington

Shields, J. E., M. E. Karr, A.R. Burden, R.W. Johnson, and J. G. Baker, (2002), “Analytic Support for the Phillips Laboratory Whole Sky Imager, 1997 - 2001”, Marine Physical Laboratory, Scripps Institution of Oceanography, University of California San Diego.

Shields, J. E., R.W. Johnson, M. E. Karr, A.R. Burden, and J. G. Baker, (2003a), “WSI Field Calibration System Operations Manual”, Marine Physical Laboratory, Scripps Institution of Oceanography, University of California San Diego, Technical Note 252, February 2003.

Shields, J. E., M. E. Karr, A.R. Burden, R.W. Johnson, and J. G. Baker, (2003b), “Analysis and Measurement of Cloud Free Line of Sight and Related Cloud Statistical Behavior – Published as Final Report for ONR Contract N00014-97-D-0350 DO #2”, Marine Physical Laboratory, Scripps Institution of Oceanography, University of California San Diego, Technical Note 262, June 2003.

Shields, J. E., R. W. Johnson, M. E. Karr, A. R. Burden, and J. G. Baker (2003c), Calibrated Fisheye Imaging Systems for Determination of Cloud Top Radiances from a UAV, International Symposium on Optical Science and Technology, SPIE the International Society for Optical Engineering, 2003.

Shields J. E., R. W. Johnson, M. E. Karr, A. R. Burden, and J. G. Baker, (2003d), Daylight Visible/NIR Whole Sky Imagers for Cloud and Radiance Monitoring in Support of UV Research Programs, International Symposium on Optical Science and Technology, SPIE the International Society for Optical Engineering, 2003.

Shields, J. E., R. W. Johnson, M. E. Karr, A. R. Burden, and J. G. Baker (2003e), Whole Sky Imagers for Real-time Cloud Assessment, Cloud Free Line of Sight Determinations and Potential Tactical Applications, The Battlespace Atmospheric and Cloud Impacts on Military Operations (BACIMO) Conference, Monterey, CA. <http://www.nrlmry.navy.mil/bacimo.html>, 2003.

Shields, J. E., A.R. Burden, M. E. Karr, R.W. Johnson, and J. G. Baker, (2004a), “Development of Techniques for Determination of Nighttime Atmospheric Transmittance and Related Analytic Support for the Whole Sky Imager – Published as Final Report for ONR Contract N00014-01-D-0043 DO #5”, Marine Physical Laboratory, Scripps Institution of Oceanography, University of California San Diego, Technical Note 263, April 2004.

Shields, J. E., M. E. Karr, A.R. Burden, R.W. Johnson, and J. G. Baker, (2004b), “Project Report for Providing Two Day/Night Whole Sky Imagers and Related Development

Work for Starfire Optical Range – Published as Final Report for ONR Contract N00014-97-D-0350 DO #6”, Marine Physical Laboratory, Scripps Institution of Oceanography, University of California San Diego, Technical Note 265, May 2004.

Shields, J. E., J. G. Baker, M. E. Karr, R. W. Johnson, and A. R. Burden, (2005a), Visibility measurements along extended paths over the ocean surface, International Symposium on Optical Science and Technology, SPIE the International Society for Optical Engineering, August 2005.

Shields, J. E., A.R. Burden, R.W. Johnson, M. E. Karr, and J. G. Baker, (2005b), “Cloud Free Line of Sight Probabilities and persistence Probabilities from Whole Sky Imager Data”, Marine Physical Laboratory, Scripps Institution of Oceanography, University of California San Diego, Technical Note 266, August 2005.

Shields, J. E., A. R. Burden, R. W. Johnson, M. E. Karr, and J. G. Baker (2005c), Measurement and Evaluation of Cloud Free Line of Sight with Digital Whole Sky Imagers, The Battlespace Atmospheric and Cloud Impacts on Military Operations (BACIMO) Conference, Monterey, CA. <http://www.nrlmry.navy.mil/bacimo.html>, 2005.

Shields, J. E., R. W. Johnson, J. G. Baker, M. E. Karr, and A. R. Burden, (2006), Multispectral scattering measurements along extended paths using an imaging system, International Symposium on Optical Science and Technology, SPIE the International Society for Optical Engineering, August 2006.

UNIVERSITY OF CALIFORNIA, SAN DIEGO

UCSD

BERKELEY • DAVIS • IRVINE • LOS ANGELES • MERCED • RIVERSIDE • SAN DIEGO • SAN FRANCISCO



SANTA BARBARA • SANTA CRUZ

MARINE PHYSICAL LABORATORY
PAULA HODGKISS, Management Services Officer
(858) 534-1788
(858) 822-0665 FAX
phodgkiss@ucsd.edu

291 ROSECRANS STREET
SAN DIEGO, CALIFORNIA 92106

May 4, 2007

Office of Naval Research
Department of the Navy
Attn: Ms. Sheila Neal, Security Officer
One Liberty Center
875 N. Randolph Street, Rm. 624B
Arlington, VA 22203

Dear Ms. Neal:

The enclosed report is being submitted for security review and distribution approval. The report is being prepared for publication as a:

Final Report for Contract N00014-01-D-0043-D04

Your immediate attention in processing this approval is appreciated. This report is pending distribution and request that you provide approval by email or fax so that immediate distribution can be made. I am sending a copy of this letter (without report) to our local ONR Administrative Contracting Officer, Mr. Lee Washington and UCSD Contracts and Grants Officer, Ms. Nancy Wilson.

Sincerely,

Paula Hodgkiss
Management Services Officer

Enclosure

1. Security Classification: **Unclassified**
2. Number of copies to be duplicated: **10**
3. **Title:** "Enhancement of Near-Real-Time Cloud Analysis and Related Analytic Support for Whole Sky Imagers," J. Shields [N00014-01-D-0043-D04]

Approved:

Sheila Neal, Contracting Office for Security Matters

Date: 5/8/07

DISTRIBUTION STATEMENT A:
APPROVED FOR PUBLIC RELEASE; DISTRIBUTION IS LIMITED

DISTRIBUTION OF TECHNICAL REPORTS AND FINAL REPORTS

N00014-01-D-0043 D004

- (1) Program Officer
Capt. Paul Stewart
Office of Naval Research, 321
Ballston Tower One
800 N. Quincy Street
Arlington, VA 22217

- (1) Lee Washington
Lead Administrative Contracting Officer (ACO/AGO)
Office of Naval Research Regional Office (ONRRO)
140 Sylvester Road, Bldg 140, Room 218
San Diego, CA 92106-3521

- (1) Director, Naval Research Laboratory
ATTN: Code 5227
Washington, D. C. 20375

- (1) Defense Technical Information Center
8725 John J. Kingman Road
STE 0944
Ft. Belvoir, VA 22060-6218
(electronic submission)